Title
Avian Responses to Mechanical Stress: Morphology and Bone Structure During Hovering, Migration, and Egg-Laying

Author
Louis, Leeann Dorothy

Publication Date
2019

Peer reviewed|Thesis/dissertation

Avian Responses to Mechanical Stress:
Morphology and Bone Structure During Hovering, Migration, and Egg-Laying

By

Leeann D. Louis

A dissertation submitted in partial satisfaction of the

requirements for the degree of

Doctor of Philosophy

in

Integrative Biology

in the

Graduate Division

of the

University of California, Berkeley

Committee in charge:

Professor Robert Dudley, Chair
Professor Tony M. Keaveny
Professor Rauri Bowie
Professor Robert J. Full

Summer 2019

Abstract

Avian Responses to Mechanical Stress:
Morphology and Bone Structure During Hovering, Migration, and Egg-Laying

by

Leeann D. Louis

Doctor of Philosophy in Integrative Biology

University of California, Berkeley

Professor Robert Dudley, Chair

All organisms experience mechanical forces which shape their body size and morphology. However, mechanical forces vary between species within a given lineage, between populations of a given species, between different sexes, and even within an individual organism over time. Here, I explore how variable mechanical forces influence bird morphology across these different scales. First, I explore how the presence or absence of hovering behavior alters bone morphology across a lineage of birds. Second, I look at how remaining sedentary or migrating influences morphology within a single species. Third, I study how egg-laying behavior alters female bone morphology over time. By studying how mechanical forces influence morphology we can gain an understanding of the mechanisms that control organism shape.

Chapter 1: Morphological Adaptations to Hovering in a Remarkable Radiation of Old World Nectar-Eating Birds: the Sunbirds (Nectariniidae)

Hovering is a unique form of locomotion that allows an animal to remain stationary in the air. While hummingbirds hover almost exclusively to obtain nectar from flowers, other nectar-eating birds vary in whether and how often they hover. This tendency may be constrained by morphology. Hummingbirds have several morphological adaptations to hovering, including long wings, short tarsi, and shortened proximal wing bones.

I hypothesized that the morphology of hovering birds converges on hummingbird morphology. Specifically, I predicted that hovering birds would be lower in mass and have longer wings, reduced tarsi, and longer tails. I also predicted that hovering birds would not vary in mass across elevations, but that higher elevation species would have relatively long wings. To test these predictions, I measured mass, elevation, wing length, tail length, and tarsus length in a group of birds that includes species that hover and species that do not hover: the sunbirds (Nectariniidae).

In contrast to my predictions, hovering sunbird species were heavier than those that did not hover. Female hovering sunbirds did have relatively long wings, but males did not. Hovering sunbirds did not have relatively short tarsi or long tails. However, male sunbirds in general did have relatively short tarsi and long tails. Hovering species did not vary in mass across elevation, Females but not males had longer wings with increasing elevation.

These results suggest that nectar-eating behavior, not hovering behavior, may select for hummingbird-like morphologies such as long wings and short tarsi. Additionally, hovering behavior seems to apply weaker selective forces on the morphology of most birds than it does in hummingbirds. A deeper understanding of the morphological requirements for hovering will aid in our understanding of the evolution of nectar-eating and its association with hovering behavior.

Chapter 2: Influence of Migratory Behavior on Bone Morphology in the Dark-Eyed Junco (*Junco hyemalis*)

Migratory behavior requires birds to expend increased energy as they spend a greater proportion of the day flying. To prepare, birds increase body mass by 20% or more, increase the masses of muscles associated with flight, and shrink organs that are not used during migration such as the stomach. This simultaneous increase in body mass, muscle mass, and the number of loads applied to the body each day has been associated with increased microcrack formation and risk of fatigue fracture in humans. Is migratory behavior in birds associated with any adaptations in bone structure?

To answer this question, I compared bone morphology of resident (*J. h. carolinensis*, *J. h. pontilis*) and migrant (*J. h. hyemalis*, *J. h. montanus*, *J. h. aikeni*) subspecies of the Dark-Eyed Junco (*Junco hyemalis*). Specifically, I looked at trabecular and cortical bone morphology in the humerus and femur using micro-computed tomography and linear mixed effects models.

I found that migratory birds had humeri that were thinner and wider, but these changes were not associated with a difference in geometric stiffness. In contrast, migratory femora were thinner, resulting in reduced geometric resistance to bending. Therefore, migrant femurs are less stiff under loading, but migrant and resident humeri have similar whole bone stiffness properties.

Taken together, these results suggest that residents and migrants have similar demands on the humerus, but that migrants have reduced demands in the femur. This may be due to resorption of muscle mass during migration, relatively increased evolutionary pressures to reduce body mass in migrants, or other differences in selection between residents and migrants. Further research should be performed to explore what mechanisms drive differences between resident and migrant birds.

Chapter 3: Microstructure and Mechanical Properties of Bird Bone During Egg-Laying

In the week prior to laying an egg, a female bird creates a unique calcified tissue inside her long bones: medullary bone. Medullary bone is primarily thought to function in calcium storage, as females draw heavily from it when producing an eggshell. However, it also increases overall bone mass and alters whole bone mechanical properties, and thus may influence avian energetics and behavior. What is the structural contribution of medullary bone to resisting forces during bending, and how might it influence behavior?

To answer this question, I gave male zebra finches (*Taeniopygia guttata*) an estrogen-eluting implant in order to generate a predictable model of medullary bone. Using micro-computed tomography scans of the humerus and femur, I created models with and without medullary bone, and used finite element analyses to apply bending forces (resulting in 1% axial displacement) and measure the load held in each bone.

I found that the addition of medullary bone resulted in a 36 – 41% increase in bone mass but an increase in whole bone stiffness of only 24 – 30%. It also had minimal influences on the load held in the cortex. I confirmed these results in similar models of female birds during egg-laying.

My results align with those of previous studies, which showed that medullary bone increases whole bone strength, but that increases are not concomitant with its increase in volume. Medullary bone therefore represents an ideal compromise between the need to store calcium for use during egg-laying while maintaining bone loading and bone mechanical integrity.

Conclusion

In summary, variations in mechanical forces influence morphology across varying scales. Specifically, the high forces experienced during hovering may select for longer wings, while the large energy expenditures during migration may select for reduced femur mass. In addition, these studies demonstrate that birds can be a useful system in which to understand how mechanical forces influence morphology. Future work should explore the nuances and potential mechanisms by which mechanical forces shape morphology.

Dedication

This dissertation is dedicated to my parents,
Mr. Richard F. Louis, Jr. & Ms. Gail Louis.

It is because of your unconditional love and hard work that I have been able to pursue what I love, believe in myself, and to achieve all that I have.
I cannot thank you enough.

Love, Dee

Table of Contents

Acknowledgements

Persevering through the successes and (many, many) failures of a dissertation is impossible without support. With this in mind, I would like to take the time to thank everyone that made my dissertation possible. I must first thank my committee, without whom I would never have learned all the hard but important lessons that made me a scientist. Many thanks to:

My adviser, Professor Robert Dudley, for giving me the freedom to study what interests me most, and for being so patient while I figured out what that is;

Professor Tony Keaveny, for reinvigorating my love of orthopedic biomechanics, for patiently teaching me how to ask and answer important questions in science, for supporting me as I applied engineering principles to my biological questions, and for believing in me and my work when I had trouble doing so myself;

Professor Rauri Bowie, for giving me the knowledge I needed to be an ornithologist, for helping me understand the behaviors that drive the morphology, for reminding me to pursue what interests me most, and for helping me understand my data; and

Professor Bob Full, for giving me my foundation in biomechanics, for pushing me to answer the most interesting questions that I can *with the data that I have*, for giving me the right advice when I needed it most, and for being a cheerleader when I needed it.

I would also like to thank many other faculty, labs, and staff at Berkeley and across the United States who have generously taught me scientific techniques or allowed me to use their resources. Many thanks to:

Professor George Bentley and everyone in his lab, particularly Dr. Kate Wilsterman, for patiently teaching me techniques in avian husbandry, for extensive use of the zebra finch colony at the field station, and for teaching me the importance of endocrinology in my research;

Professor Tyrone Hayes and everyone in his lab, particularly Mai Nguyen and Maggie Tsang, for patiently teaching me the methods of soft tissue histology, allowing me to use your space and equipment, helping me troubleshoot the many issues that came up, and being supportive of me and my work;

Terri Barclay, Carla Cicero, Ioana, and the Museum of Vertebrate Zoology Prep Lab for patiently teaching me how to prepare museum quality bird skins, and for many wonderful evenings preparing specimens together;

Tanya Garcia-Nolen and the UC Davis Veterinary Orthopedic Laboratory, for training me in using your micro-computed tomography scanner and in using your hard tissue histology facilities, and for allowing me to use those facilities extensively;

Dula Parkinson at the Advanced Light Source at Lawrence Berkeley National Laboratory, for helping me obtain the best tomographic data possible, and for staying late to ensure I got the data that I needed;

Professor Marian Young and her group at the National Institute of Dental and Craniofacial Research, especially Vardit Kram, for extensive use of your micro-computed tomography facility, for generously helping me when issues came up, and for showing a true interest in my work;

Professor X. Edward Guo and his group at Columbia University, particularly Samuel Robinson, for giving me time on your micro-computed tomography machine and helping me troubleshoot issues;

Professor Larry Suva and his lab at Texas A&M, for helping me hone my bone histology knowledge and skills;

And the American Museum of Natural History Department of Ornithology, especially Tom Trombone, Bentley Bird, Paul Sweet, and Peter Capainolo, for loaning me many sunbird and Dark-Eyed Junco specimens, and for permitting me to visit the museum.

I would also like to thank the amazing and brilliant undergraduates who have contributed their hard work to my research over the years, particularly:

Amanda Torres in Integrative Biology, who spent 2 years helping me measure bird bones, perform delicate dissections to remove bones, and perform background research in endocrinology;

Cy David in Earth and Planetary Science, who wrote critical code for my work on sunbirds and with whom I had many useful research conversations;

Edric Balallo in Molecular and Cellular Biology, who spent a year supervising egg counts at the field station, performing dissections, and doing many other essential lab tasks that helped me focus on my science; and

Grace Wang in Integrative Biology, who spent a year helping me do micro-computed tomography scans all the way in Davis.

Jason Zhou in Bioengineering, who designed holders and scanning sheets to streamline my micro-computed tomography scanning process;

Eshan Nirody in Molecular and Cellular Biology, who wrote critical code for my studies in bone porosity;

Leo Brossollet in Mechanical Engineering, who designed and built my holders for mechanical testing bird bones in 2016; and

Jessica Chiu in Mechanical Engineering, who helped me troubleshoot my first experiment with hummingbirds in 2014.

The colleagues and friends that I have met along this journey are a big part of why I have felt so welcomed in the fields of biomechanics bone biology. Thanks especially to:

The Dudley Lab, especially Ashley Smiley, Alejo Rico-Guevara, Erik Sathe, Marc Badger, and Sofia Chang, with whom I have shared so many celebrations, stories, and scientific discourses;

Saghi Sadoughi, who befriended me during the World Congress on Biomechanics and at the American Society of Bone and Mineral Research in 2018; you are a brilliant and thoughtful scientist and truly made me feel like I belonged in bone biology;

Noah Bonnheim, who has been my amazing and thoughtful collaborator in our research on medullary bone, who helped me feel welcome on Prof. Tony Keaveny's lab, and who has helped me validate my knowledge in materials science and bone biology; and

Tom Libby, who gave me critical feedback on the designs of my bone holders, helped me practice and reinforce my knowledge of solid mechanics when I needed it; trained me to use the laser cutter, 3D printer, bandsaw, and other equipment in the Center for Integrative Biomechanics in Education & Research; and with whom I had many wonderful conversations about biomechanics and engineering; and

Many faculty at UC Berkeley who helped me grow as a scientist: Professor Marvalee Wake for helping me use and interpret my histological data; Professor Michael Nachman for helping me learn the nuances of academic hiring; Professor Lisa Pruitt for helping me truly understand materials science and use it in my work; Professors David Ackerly, Brent Mishler, and Kip Will for giving me a strong foundation in phylogenetics; Professors Noah Whiteman,

Eileen Lacey, and Tyrone Hayes for helpful talks about diversity in academia; and generous support from many other faculty members in the Departments of Integrative Biology, Mechanical Engineering, and Environmental Science, Policy, and Management.

Many people gave me encouragement and support during my dissertation, without which I could never have gotten this far. Huge, huge thanks to:

Professor Mary Bouxsein at Harvard Medical School. The time I spent in your lab gave me many of the core skills in bone biomechanics that I used to form the core of my dissertation. Our conversations sparked ideas that kept me going in my research, reminded me that my work is interesting and valuable, and helped me believe in myself. I would not be here without you.

My good friend Erin Brandt. You have been with me all 6 years of my dissertation, and have seen me through some of my toughest times. Thank you for being my study buddy, research buddy, and now writing buddy. Thank you for spending countless hours listening to me work through the stressors of graduate school (and life), for providing some of the best writing advise I have ever received, and for being a steadfast friend. I will truly miss you, but I am glad we had this journey together.

My Mom and Dad, Mr. Richard F. Louis, Jr. & Ms. Gail Louis. You have worked so hard to create a safe, loving home, and I feel lucky every day for this. Thank you for believing in me and my work all these years, for trusting my decisions, and for being some of the most loving, kind, and hardworking people I know.

My Grandma, Ms. Patricia Louis, for reminding me to be thankful for my health and happiness every week, for many fun visits and family memories, and for supporting my family all these years. I love you and miss you.

My amazing sisters, Jeanette Kaczmarkiewicz and Kim Louis. You have always, always been there for me, listened to me, and been so supportive. You understand me better than anyone, and always know what to say to help me feel better. You are my best friends, and I couldn't ask for any better.

Margaret Tzen and her amazing family: Victor, Walter, and Dorothea, as well as her parents. Thank you for welcoming me into your family and for sharing your love and faith. I always feel restored after spending time with you, and feel so lucky that you could be my family away from home during my time at Cal.

Ashley Smiley. Thank you for being an open and honest friend, and for sharing so many sammies and for always being available to chat, go for a walk, or have a coffee. Thank you especially for awakening me to the inequities in academia; I have worked to show others the same ever since.

Rob Matthew. Thank you for always supporting me, whether to brainstorm research ideas or decompress by camping or making beer.

And thank you to all my amazing friends who have supported me along the way: Anjuli Kannan, Matt Medeiros, Diego Mena, Lena Sawin, Meg Dowd, Miranda Dobbs, Adam Diorio, Therese LaMarche, and Melisa Pendergrass.

Finally, thank you to all of the funding sources that have supported my research over the years: the National Science Foundation (NSF) Graduate Research Fellowship Program, the NSF Integrative Graduate Education and Research Traineeship program, the American Society of Bone and Mineral Research, the Society of Integrative and Comparative Biology, the American Ornithologists' Union, the American Museum of Natural History, the Lawrence Berkeley

National Lab Advanced User Facility, the UC Berkeley Sigma Xi Foundation, the UC Berkeley Museum of Vertebrate Zoology, and the UC Berkeley Department of Integrative Biology.

Curriculum Vitae

leeann.louis@gmail.com ● 914-420-3742 ● LinkedIn: https://www.linkedin.com/in/leeannlouis/

EDUCATION

University of California, Berkeley. Expected 08/2019
Ph.D. Candidate Integrative Biology. GPA: 4.0.
Dissertation: Avian Responses to Mechanical Stress: Morphology and Bone Structure During Hovering, Migration, and Egg-Laying

Cornell University 05/2009
B.S. Biological Engineering. GPA: 3.5. *Cum laude.*

RESEARCH EXPERIENCE

Graduate Researcher, Dept. of Integrative Biology, University of California, Berkeley
PI: Prof. Robert Dudley, Ph.D. 08/2013 – 08/2019

- Develop novel avian animal model to study how bone adapts to repeated high-stress loading (migratory birds) and massive calcium draws (egg-laying birds).
- Interpret micro-computed tomography (CT) data of bone to deduce adaptations to altered loading.
- Collaborate with 2 engineers and a veterinary researcher to study a novel bone tissue.
- Establish and lead 3 independent research projects, including acquiring funding.
- Analyze micro-CT data of 700+ animals using image analyses and statistics (Scanco, MATLAB, R).
- Report research findings through frequent reports, 20 presentations, and 4 manuscripts (in prep).
- Train and manage up to 3 concurrent lab assistants.

Research Assistant, Dept. of Orthopedics, Harvard Medical School, Boston, MA
PI: Mary L. Bouxsein, Ph.D. 08/2010 – 08/2012

- Used preclinical imaging to study the influence of reduced loading, diabetes, and sclerostin on bone.
- Collected and analyzed CT data (Scanco) from 500+ animals, resulting in 8 publications.
- Created a database to manage medical research projects, reducing missed deadlines.
- Reported findings to clients and collaborators through presentations and reports.
- Performed husbandry, including colony management, in vivo x-rays, and injections.

Research Assistant, Cornell University Laboratory of Ornithology, Ithaca, NY
PI: Kimberly Bostwick, Ph.D. 08/2006 – 08/2010

- Developed novel methodology to visualize feathers using CT and iodine staining.
- Created finite element models of skulls using CT data, Aviso, and Strand7, resulting in a publication.

FELLOWSHIPS, GRANTS, & AWARDS

Fellowships:

National Science Foundation Graduate Research Fellowship Program	2013 – 2018
National Science Foundation Integrative Graduate Education and Research Traineeship in Integrative Biomechanics	2013 – 2015

External Grants:

American Society of Bone and Mineral Research Adele L. Boskey Young Investigator Award ($1,000)	2018
Society of Integrative and Comparative Biology Grants-in-Aid-of-Research ($1,000)	2018
American Ornithologist's Union Research Award ($2,343)	2015
American Museum of Natural History Collection Study Grant ($750)	2015

Internal Grants:

UC Berkeley Sigma Xi Grants-in-Aid of Research ($300)	2019
UC Berkeley Museum of Vertebrate Zoology Student Research Funds ($4,500 total)	2015 – 2019
UC Berkeley Department of Integrative Biology Summer Research Grants ($7,732 total)	2015 – 2018

Awards:

UC Berkeley Department of Integrative Biology Dissertation Completion Award. Given to an outstanding graduate student during their last semester	2019
General User & Rapid Access Proposals to use the Lawrence Berkeley National Lab Advanced User Facility Beamline 8.3.2: Tomography (Nine 8-hour shifts)	2017 – 2019

PUBLICATIONS

Devlin MJ, Robbins A, Cosman MN, Moursi CA, Cloutier AM, **Louis L,** Van Vliet M, Conlon C, Bouxsein ML. Differential effects of high fat diet and diet-induced obesity on skeletal acquisition in female C57BL/6J vs. FVB/NJ Mice. Bone Reports. 2018;8:204-214.

Spatz JM, Ellman R, Cloutier AM, **Louis L,** van Vliet M, Dwyer D, Stolina M, Ke HZ, Bouxsein ML. Sclerostin antibody inhibits skeletal deterioration in mice exposed to partial weight-bearing. Life Sciences in Space Research. 2017;12:32-38.

Devlin MJ, Brooks DJ, Conlon C, van Vleit M, **Louis L**, Rosen CJ, Bouxsein ML. Daily leptin blunts marrow fat but does not impact bone mass in calorie restricted mice. Journal of Endocrinology. 2016;229:295-306.

Devlin MJ, Van Vliet M, Motyl K, Karim L, Brooks DJ, **Louis L,** Conlon C, Rosen CJ, Bouxsein ML. Early-onset Type 2 Diabetes impairs skeletal acquisition in the male TALLYHO/JngJ Mouse. Endocrinology. 2014;155:3806-3816.

Zhu ED, **Louis L**, Brooks DJ, Bouxsein ML, Demay MB. Effects of bisphosphonates on the rapidly growing male murine skeleton. Endocrinology. 2014;155:1188-1196.

Bernhard JM, Edgcomb VP, Visscher PT, McIntyre-Wressig A, Summons RE, Bouxsein ML, **Louis L**, Jeglinski M. Insights into foraminiferal influences on microfabrics of microbialites at Highborne Cay, Bahamas. Proceedings of the National Academy of Sciences. 2013;110:9830-9834.

Devlin MJ, Grasemann C, Cloutier AM, **Louis L**, Alm C, Palmert M, Bouxsein ML. Maternal perinatal diet induces developmental programming of bone architecture. Journal of Endocrinology. 2013;217:69-81.

Spatz JM, Ellman R, Cloutier AM, **Louis L**, van Vliet M, Suva LJ, Dwyer D, Stolina M, Ke HZ, Bouxsein ML. Sclerostin antibody inhibits skeletal deterioration due to reduced mechanical loading. Journal of Bone and Mineral Research. 2013;28:865-874.

Lane SW, De Vita S, Alexander KA, Karaman R, Milsom MD, Dorrance AM, Purdon A, **Louis L**, Bouxsein ML, Williams DA. Rac signaling in osteoblastic cells in required for normal bone development but is dispensable for hematopoietic development. Blood. 2012;119:736-744.

Slater GJ, Figueirido B, **Louis L**, Yang P, Van Valkenburgh B. Biomechanical consequences of rapid evolution in the polar bear lineage. PLOS One. 2010;5:e13870.

SELECTED PRESENTATIONS

Louis L, Keaveny TM, Bentley GE, Dudley R. Influence of laying an egg on bird bone. Society of Integrative and Comparative Biology Annual Meeting 2019. Oral Presentation. January 5, 2019.

Louis LD, Bowie RCK, Dudley R. Skeletal morphology of migratory and resident Dark-Eyed Juncos (*Junco hyemalis*). Society of Integrative and Comparative Biology Annual Meeting 2019. Poster Presentation. January 5, 2019.

Louis LD, Keaveny TM, Bentley GE, Dudley R. Morphology of bird bone during egg-laying. American Society of Bone and Mineral Research 2018. Poster Presentation. October 1, 2018.

Louis L, Keaveny T, Bentley G, Dudley R. Morphology of bird bone during egg-laying. World Congress of Biomechanics 2018. Poster Presentation. July 12, 2018.

Louis LD, Bowie RCK, Dudley R. Morphological adaptations to hovering in a taxon of Old World nectarivorous birds: the sunbirds. Society of Integrative and Comparative Biology Annual Meeting 2018. Oral Presentation. January 7, 2018.

Louis LD, Badger MA, Dudley R. It's a breeze: aperture negotiation by hummingbirds flying into and against the wind. Society of Integrative and Comparative Biology Annual Meeting 2016. Poster Presentation. January 5, 2016.

INDUSTRY EXPERIENCE

Consultant, Biotech Connection Bay Area, San Francisco, CA 06/2018 – 09/2018

- Create slide deck to guide a client to market entry with fellow PhDs and scientists.
- Perform knowledge and opinion leader (KOL) calls and market research on immunoassays.

Project Co-Leader, Bay Area Bridge to Biotechnology, Berkeley, CA 03/2018 – 05/2018

- Collaborate with fellow PhD candidates to perform due diligence in oncology therapeutics.
- Pitch cancer therapeutics startup to venture capitalists including 5AM, Lux, 8VC, General Catalyst.

TEACHING & MENTORING EXPERIENCE

Graduate Student Instructor, University of California, Berkeley

IB 135: Mechanisms of Organisms — Spring 2016
Lead discussion sections, review material, develop lessons and worksheets.

IB 131L: Human Anatomy Laboratory — Fall 2017 & 2018
Teach cadaver and histology lab, lead 3 assistants, create and grade exams

IB 132L: Human Physiology Laboratory — Spring 2019
Run labs teaching use of blood pressure monitors, EKG, EMG; guide independent work

Mentor, Undergraduate Research Apprenticeship Program

Trained students in bone biology skills (CT scanning & analysis, dissection, lab work, MATLAB)

- Edric Balallo, Molecular and Cellular Biology — 02/2018 – 12/2018
- Cy David, Earth and Planetary Science — 02/2018 – 12/2018
- Grace Wang, Integrative Biology — 02/2018 – 08/2018
- Jason Zhou, Bioengineering — 02/2017 – 08/2017
- Eshan Nirody, Molecular and Cellular Biology — 02/2017 – 08/2017
- Amanda Torres, Integrative Biology — 02/2016 – 05/2017
- Leo Brossollet, Mechanical Engineering — 02/2016 – 05/2016
- Jessica Chiu, Mechanical Engineering — 09/2014 – 05/2015

Advanced Naturalist, Audubon Center of the North Woods, Sandstone, MN
08/2012 – 06/2013
Taught diverse groups of K-12 students hands-on lessons in teamwork and self-awareness.

SERVICE & VOLUNTEERING

UNIVERSITY SERVICE

Committee Member, Integrative Biology Faculty Search Committee. 2018
Proactively represent the graduate student voice, lead student lunches, read all applications, participate in all decisions.

OUTREACH

Instructor, Bay Area Scientists in Schools — 2013 – 2017
Teach engineering lessons to local 2nd graders.

Volunteer, California Raptor Center — 2016
Cared for and handled injured birds of prey.

Mentor, Be A Scientist Program — 2015
Mentor local 7th graders in developing science projects.

Volunteer, Museum of Science 2012
Give groups of 2nd graders personalized tours of the museum
Volunteer, Horizons for Homeless Children 2011 – 2012
Manage groups of homeless toddlers.

REFERENCES

Tony M. Keaveny
Professor, Mechanical Engineering and Bioengineering
510.390.1626
University of California, Berkeley
tonykeaveny@berkeley.edu

Robert Dudley
Department Chair & Professor, Integrative Biology
510.642.1555
University of California, Berkeley
wings@berkeley.edu

Rauri C.K. Bowie
Professor, Integrative Biology & Curator of Birds, Museum of Vertebrate Zoology
510.643.1617
University of California, Berkeley
bowie@berkeley.edu

Chapter 1. Morphological Adaptations to Hovering in a Remarkable Radiation of Old World Nectar-Eating Birds: the Sunbirds (Nectariniidae)

Introduction

Hovering flight is ubiquitous in hummingbirds but is also common in many small birds. These include a third of sunbirds (Nectariniidae) (Cheke and Mann, 2001), some flowerpeckers (Dicaeidae) (Cheke and Mann, 2001; Cheke and Mann, 2008a), some honeyeaters (Meliphagidae) (Higgins et al., 2008), a sugarbird (Promeropidae) (Cheke and Mann, 2001), and evidence in some sparrows, finches, white-eyes, and others (Brown, 1963; Wester, 2013a). Despite its prevalence, hovering is an energetically expensive form of flight. It requires birds to produce a sufficient downward momentum of air to offset their weight without the advantage of air accelerating over the wing during forward flight (Norberg, 1990), and requires a high mass-specific rate of oxygen consumption (Suarez et al., 1991). There are two general methods that birds use to hover: symmetric hovering, which is primarily used in hummingbirds; and asymmetric hovering, which is used by most other birds (Norberg, 1990). In contrast to the symmetric hovering of hummingbirds and despite the prevalence of asymmetric hovering across birds, little is known about asymmetric hovering and any morphological adaptations birds require to perform the behavior.

Symmetric and asymmetric hovering require very different wing kinematics and aerodynamics. In symmetric hovering, hummingbirds move their wings through a primarily horizontal stroke plane, thus producing aerodynamic force during both downstroke and upstroke (Ingersoll et al., 2018). In contrast, when birds other than hummingbirds perform slow-flying or hovering flight, they do not produce significant aerodynamic lift during upstroke (Chang et al., 2011; Chang et al., 2013; Muijres et al., 2012). These aerodynamic differences presumably select for different morphological adaptations to optimize their aerodynamic efficiency.

In addition, whereas hummingbirds hover almost exculsively, asymmetrically hovering species vary widely in the frequency with which they employ hovering flight. Wester (2013a) reviewed evidence of hovering behavior across passerine birds and categorized the frequency with which species were found to hover, including descriptions such as often, exclusively, sometimes, and rarely. They also note that hovering frequency varies within species based on the type of flower visited. Here, I was broadly interested in whether morphology varies with hovering ability. Therefore, I treated hovering as a binary trait, and separated species into those that are known to hover and those that re not known to hover (e.g. hovering presence and hovering absence, respectively).

Hummingbirds have many morphological adaptations associated with hovering: drastically shortened proximal wing bones to increase wingtip speed (Zusi 2013), wings that scale in length with their body mass faster (α mass$^{2/3}$) than what is seen in other birds (α mass$^{1/3}$) (Greenewalt, 1962; Skandalis et al., 2017), aerodynamic constraints on upper body mass (Hainsworth and Wolf, 1972), and reduced tarsus length (Collins and Paton, 1989). We also know that hummingbirds do not vary in mass across elevation (Skandalis et al., 2017), but that individuals

living at higher elevations have larger wings for their mass than birds at lower elevations (Altshuler and Dudley, 2002; Skandalis et al., 2017). This trend of increased wing length with elevation is not unique to hummingbirds (Hamilton, 1961; Traylor, 1950), but hummingbirds are among the species that demonstrate it. Regarding tail length, Clark and Dudley (2009) found that removing or extending the tail of Anna's hummingbirds (*Calypte anna*) does not influence the metabolic costs of hovering flight. However, hummingbird tail length does scale with positive allometry (α mass$^{1/2}$), similar to wing length (Clark, 2010), and a long tail has been found to assist in pitch stability in hovering hummingbirds (Altshuler et al., 2009), suggesting that a long tail may be beneficial in slow and hovering flight (Thomas and Balmford, 1995). Given our knowledge of the morphological adaptations of symmetrically hovering hummingbirds to their flight behavior, it is surprising how little we know about any morphological adaptations that might exist for asymmetric hovering.

Therefore, I asked the question: does asymmetric hovering select for specific morphological adaptations? To address this question, I look at a group of birds in which asymmetric hovering behavior is known (the sunbirds, Nectariniidae) and demonstrate using ancestral reconstruction that hovering behavior has appeared numerous times. To derive predictions about what morphological trends I expect to see with asymmetric hovering behavior, I make the broad hypothesis that that hovering sunbird species converge morphologically on features seen in hummingbirds. Given this hypothesis, and the observation about morphological trends in hummingbirds discussed above, I can make 5 predictions: (1) hovering sunbirds will tend to be slightly lower in mass than non-hovering sunbirds; (2) hovering sunbirds will demonstrate wing length hyper-allometry, that is, wing length will that scale at an exponent larger than 1/3 for hovering sunbirds; (3) hovering sunbirds will have reduced tarsal length compared to non-hovering sunbirds; (4) sunbirds will not differ in mass across elevation; and (5) wing length will increase with elevation in hovering sunbirds are longer at higher elevations than in non-hovering sunbirds. Additionally, given that a long tail seems to benefit hovering hummingbirds, and given that it aids in pitch stability in Japanese White-Eyes (*Zosterops japonicus*) (Su et al., 2011; Su et al., 2012), I predict that (6) tail length will scale with positive allometry in hovering sunbirds.

Methods

Literature survey

An exhaustive search of the literature was performed to collect all available data on sunbird hovering behavior, elevational range, and morphology.

Hovering behavior was treated as a binary variable for each species. The general literature on sunbird behavior was combed for any mention of hovering behavior (Cheke and Mann, 2001; Cheke and Mann, 2008b; Wester, 2013b). Mention of hovering behavior was coded as presence and lack of mention was coded as absence. Two authors (Louis and Torres) independently scanned the literature to ensure that coding was accurate.

Data on minimum, maximum, and midpoint elevation (halfway between minimum and maximum), were taken from Cheke and Mann (2001) and from the Handbook of Birds of the World (Cheke and Mann, 2008b). Where data on multiple subspecies existed, the overall range for all subspecies was used. In the few cases where data from the two sources differed, the data

from the Handbook was used. Two authors (Louis and Torres) independently scanned the literature to ensure that coding was accurate.

Mass data were obtained from the CRC Handbook of Avian Body Masses (Dunning, 2008) and supplemented with data from Cheke and Mann (2001) on the few occasions where the CRC Handbook did not have data. Lengths of the wing, tail, and tarsus were obtained from the literature (Cheke and Mann, 2001). Where data for multiple subspecies existed the subspecies for which there was also mass data was used. If there was no mass data, the subspecies with the largest sample size was used. For all data, male and female values were recorded separately, and species averages represent the average of the male and female average. Data were $\log_{10}$ transformed prior to allometric analyses.

Morphological measurements

In order to validate morphological data compiled from the literature, direct measurements were taken from 2388 specimens representing 113 species housed in 11 different museums: American Museum of Natural History, New York; British Museum of Natural History, London; Carnegie Museum of Natural History, Pittsburgh; Delaware Museum of Natural History, Wilmington; Field Museum of Natural History; Muséum National d'Histoire Naturelle, Paris; Royal Museum for Central Africa, Tervuren, Belgium; National Museums of Kenya, Nairobi; Swedish Museum of Natural History, Stockholm; National Museum of Natural History, Smithsonian Institution, Washington, D.C.; and Zoological Museum, University of Copenhagen, Denmark. Measurements were performed by one person (R. C. K. B.) as detailed elsewhere (Bowie et al., 2004; Bowie et al., 2016). Briefly, the following morphological measurements were taken of each specimen: wing length (with the wing flattened and measured from the carpal joint to the tip of the longest primary feather), length of the shortest tail feather (measured from the base of the pygostyle to the tip of the central or outer rectrix), and tarsus length. Wing length was measured to the nearest 0.5 mm with a wing rule, all other measurements were taken using Vernier calipers to the nearest 0.1 mm. Data on the elevation at which the specimen was collected and the mass at collection were also included where available.

Phylogenetic analyses

Both ancestral state reconstructions and phylogenetic comparative analyses were performed in R version 3.5.1 (R Core Team, 2018) using a time-calibrated phylogeny of sunbirds provided by R. C. K. Bowie (pers. comm.). Prior to analyses, the tree was converted to an ultrametric format using the *chronopl* function in *ape* (Paradis et al., 2004) and a smoothing parameter (lambda) of 1. To determine the ancestral state of hovering behavior, trait evolution was modeled using a continuous time Markov model implemented via implementation of the *ace* function in *ape*. Four evolutionary models were tested: 1) an equal rates model, where it is equally likely to transition from non-hovering to hovering as the reverse, 2) a different rates model, where the rates of transition from non-hovering to hovering are different from the reverse, a 3) an irreversible model where only transitions from non-hovering to hovering are allowed, and 4) an irreversible model where only transitions from hovering to non-hovering are allowed. The best model was identified using the second order Akaike Information Criterion (ΔAICc) to take sample size into account (Burnham and Anderson, 2002; Posada, 1998; Posada and Buckley, 2004). This model was then simulated 1,000 times using the *make.simmap* function in phytools (Bollback, 2006; Revell, 2012; Revell, 2013). The summary of this simulation was then used to determine the

state of the base of the tree and to find the rate of transitions between behavior types. Then the probability of the hovering state at each ancestral node of the tree was mapped using the *make.simmap* and *plotSimmap* functions, also in *phytools* (Revell, 2012; Revell, 2013).

Morphological analyses

Comparative analyses were performed on data from the literature and on the data collected by R. C. K. B. using phylogenetic generalized least squares (PGLS). Prior to these analyses, species without data were pruned from the phylogeny using *ape* (Paradis et al., 2004). This resulted in varying sample sizes for each analysis, which are noted in the results. When data collected by R. C. K. B. was used, data were weighed by the sample number and standard error$^{-1/2}$ for the predictor using the *varFixed* function. Additionally, when an analysis modeled a morphological variable (wing length, tail length, tarsus length) against mass, both variables were log-transformed prior to analyses.

Testing model fit. PGLS runs an ordinary least squares regression but varies the covariance matrix such that it is modified based on the phylogeny (Martins and Hansen, 1997; Symonds and Blomberg, 2014). However, the way in which the phylogeny is modified depends on the evolutionary model that is assumed. As such, three different evolutionary models were tested for each morphological outcome variable: (1) Brownian motion, the simplest model, which assumes that a trait varies randomly over time; (2) Pagel's λ, which uses Brownian motion but adds a branch length scaling factor λ, which can vary between 0 (phylogeny does not influence the data) and 1 (data follows true Brownian motion across the phylogeny) (Freckleton et al., 2002; Pagel, 1999); and (3) Ornstein-Uhlenbeck, a Brownian-like model that models stabilizing selection by using an additional parameter that measures movement towards an optimum value (Hansen, 2006). These models were tested using, respectively, the *corBrownian*, *corPagel*, and *corMartins* functions all implemented via the *ape* software package (Paradis et al., 2004). In addition to testing three evolutionary models, several dependent variables were included in each model to determine whether they contributed to the variance of a given morphological outcome. Specifically, models were tested that (1) modeled the morphological outcome as a constant, e.g. assumed that no variables contributed significantly to its variance; (2) only included mass; (3) only included hovering behavior; and (4) only included elevation. Additionally, additive and interaction models were tested that included mass and hovering behavior (5 & 6); mass and elevation (7 & 8); and mass, hovering behavior, and elevation (9 & 10). For all models, ΔAICc was calculated and compared to determine model fit using the *AICc* function in the *AICcmodavg* package.

Species dimorphism. To determine the relationship between morphology and mass, analyses of mass dimorphism were performed. For both the literature dataset and the dataset collected by R. C. K. B., the difference in mass between males and females was compared with the hypothesis that it is 0 using PGLS. Then, PGLS was performed using the log-transformed data, and the slope of each resulting relationship was compared with the slope predicted under geometric similarity (e.g. length α mass$^{1/3}$) using a Student's t-test. To determine if significant dimorphism existed between males and females, PGLS was first performed separately on each sex. Then, a t-test was performed to determine if the slope and intercept differed from each other.

Morphology, hovering behavior, and elevation. To determine if hovering or elevation explained any of the variation in morphology, two approaches were used: first, PGLS analyses were re-run including additive and interaction terms for hovering or elevation as a covariate. The slope of each resulting relationship was compared with the slope predicted under geometric similarity (e.g. length α mass$^{1/3}$) using a Student's t-test. Second, size-corrected residuals were used. Specifically, the log-transformed residuals of wing length, tail length, and tarsus length against body mass were found using the function *phyl.resid* in *phytools* (Revell, 2009). Then residuals were regressed against the hovering trait or against elevation as predictions required.

Results

The literature included data on 124 species, of which 102 were contained in the phylogeny. The data collected by R. C. K. B. included 101 species, of which 85 were contained in the phylogeny.

Phylogenetic analyses

Three of the four ancestral state reconstruction models were close fits for the evolution of hovering behavior: the equal rates model (ΔAICc = 0.00), the different rates model (ΔAICc = 0.54), and the irreversible model in which only transitions from hovering to non-hovering were allowed (ΔAICc = 1.12). The irreversible model in which only transitions from non-hovering to hovering was a much poorer fit (ΔAICc = 9.25). Using the equal rates model, stochastic character mapping of the hovering behavior showed that that transitions between hovering behavior types are common (**Error! Reference source not found.**). Trees had an average of 43.65 changes between states; 24.74 from non-hovering to hovering and 18.92 from hovering to non-hovering. Based on stochastic character mapping, the ancestral state of the base of the sunbird tree was likely a non-hoverer (non-hoverer: 0.982, hoverer: 0.018).

Morphological analyses

Testing model fit. Wing length, tail length, and tarsus length were modeled for males and females using three evolutionary models (Brownian motion, Pagel's λ, and Ornstein-Uhlenbeck) and 10 combinations of explanatory variables (including mass, hovering behavior, and elevation) (Tables

). Four of 6 morphology-sex outcomes (female wing length, female tail length, and male and female tarsus length) were best fit by a model including mass only. Male wing length was best fit by an additive model including mass and elevation. Male tail length was best fit by a constant. Brownian motion was the best evolutionary model for 3 of the 6 morphology-sex outcomes (female wing length, male and female tarsus length), Pagel's λ was the best fit for 2 of the outcomes (male wing length and female tail length), and Ornstein-Uhlenbeck best fit male tail length only. However, all three models of evolution produced competitive models for all morphology-sex outcomes. Given that all models of evolution were competitive, and given that morphology may be undergoing some directional selection, I used the Ornstein-Uhlenbeck correlation method for all of the following models. However, it should be noted that Brownian and Pagel's λ methods were also tested and produced similar results to those discussed below.

Species dimorphism. Based on the literature data, males are significantly heavier than females (n = 49, males: 10.69 g, females: 9.43 g, p = 0.023). Results from the data collected by R. C. K. B. also showed that males were heavier, but the difference was not significant (n = 10, males: 9.37 g, females: 8.19 g, p = 0.192). Wing length, tail length, and tarsus length for both males and females were significantly correlated with mass when both literature data and data collected by R. C. K. B. were used with three exceptions: the literature data for tail length in males, and the R. C. K. B. data for tail length and tarsus length in females (**Error! Reference source not found.**). The latter two trends could be explained by small sample size: there were only 6 and 4 species available for female tail length and tarsus length, respectively. The lack of correlation between tail length in males and mass may be because literature data only included the long tails present under sexual selection. For the morphological outcomes that did correlate with mass, the estimated slope did not differ from what is predicted under geometric similarity except for in the literature data for tarsus length in males, which showed a significantly smaller slope than predicted (0.165 ± 0.066 mm, p = 0.017). Males and females did not differ in significantly in intercept or slope for any relationship.

Morphology and hovering behavior. Hovering species tended to be heavier in both males (non-hovering: 9.96 g, hovering: 11.29 g) and females (non-hovering: 8.82 g, hovering: 9.93 g) in the literature data, but PGLS indicated that the differences were not significant (p_{males} = 0.243, $p_{females}$ = 0.234). The data collected by R. C. K. B. showed similar results: hoverers were heavier in both males (non-hovering: 8.33 g, hovering: 9.43 g) and females (non-hovering: 7.79 g, hovering: 9.24 g), but the differences were not significant (p_{males} = 0.373, $p_{females}$ = 0.536). Hovering did not contribute significantly to wing, tail, or tarsus length morphology in males or females (**Error! Reference source not found.**, **Error! Reference source not found.**). The only exception was for the literature data for female wing length, where hovering behavior decreased the intercept (-0.261 ± 0.122 mm, p = 0.038) and increased the slope (0.115 ± 0.05 mm, p = 0.043).

Morphology and elevation. Sunbirds species (n=98) live at an average midpoint elevation of 1143 m, an average maximum elevation of 1964 m, and an average elevational range of 1644 m (**Error! Reference source not found.**). Hovering sunbird species tend to live at higher midpoint elevations (n = 47, 1173 m) than non-hovering species (n = 37, 1140 m), but the difference is not significant (p = 0.316). However, hovering species do live at significantly higher maximum elevations (non-hovering: 1901 m, hovering: 2094 m, p = 0.011), and over larger elevational ranges (non-hovering: 1523 m, hovering: 1842 m, p < 0.001). Mass did not correlate with midpoint elevation, maximum elevation, or elevational range for males or females. Elevation did not contribute significantly to wing, tail, or tarsus length morphology in males or females (**Error! Reference source not found.**). The only exception was for the literature data for female wing length, where elevation increased the intercept (0.198 ± 0.093 mm length / km elevation, p = 0.040).

Discussion

To determine whether the morphology of asymmetrically hovering birds is similar to the morphology of symmetrically hovering hummingbirds, I analyzed trends in wing, tail, and tarsus length with mass, hovering behavior, and elevation in a diverse group of variably asymmetric hovering birds: the sunbirds. I hypothesized that hovering sunbird species converge

morphologically on features seen in hummingbirds. Below, I review the predictions I made as a result of this hypothesis, discuss whether my data support these predictions, and interpret my findings in the context of sunbird ecology.

Hovering sunbirds are not lighter

Since hummingbirds tend to be aerodynamically restricted in mass (Hainsworth and Wolf, 1972), I predicted that (1) hovering sunbirds would be lower in mass than sunbirds that do not hover. In contrast, hovering sunbirds tended to be heavier (reject prediction 1). The heaviest sunbird used in this analysis was 16.7 g, which is less than the mass of the heaviest known hummingbird (*Patagona gigas*, 20.2 g (Dunning, 2008)). Thus, the sunbirds used in this analysis are within the aerodynamic constraints on mass created by hovering. This may remove the need for hovering species to be lower in mass and allow mass to be selected by other features of ecology, such as elevation or interspecies dominance (Collins and Paton, 1989).

Female hovering sunbirds have longer wings

Additionally, I predicted that like hummingbirds (Greenewalt, 1962; Skandalis et al., 2017), (2) hovering sunbirds would have long wings for their mass in order to accommodate the large induced power requirements of hovering flight. I found support for this prediction in females, as hovering behavior increased the slope of the relationship between log-transformed wing length and log-transformed mass (partially accept prediction 2). This suggests that hovering behavior may indeed require an increase in wing length. However, given the lack of nuance used to define hovering behavior in this study, further study should be performed to confirm this relationship. Across sunbirds in general, both male and female sunbird wing lengths scaled with body mass$^{1/3}$. This matches what we see in most bird species, and contrasts with the relationship of wing length α body mass$^{2/3}$, which we see in hummingbirds (Greenewalt, 1962). These findings indicate that asymmetric hovering behavior may select for longer wings in sunbirds, but that nectar-eating in general does not require the exceptionally long wings that we see in hummingbirds. However, this study did not include information about wing area. Work by Greenewalt (1975) showed that wing area α body mass$^{1.000}$ for hummingbirds, while for passerines wing area α body mass$^{1.275}$. Since wing length scales in sunbirds at approximately body mass$^{1/3}$, this suggests that sunbirds have more rounded wings than hummingbirds. Future work should explore sunbird wing area and wing shape in relation to hovering behavior, and associate wing length and area with more quantitative measures of hovering behavior, such as the length of time individuals of a given species and with a given wing length can hover and the tendency or frequency with which individuals in a given species choose to hover.

Hovering sunbirds do not have shortened tarsi

Given that hummingbirds have relatively short tarsi for their mass (Collins and Paton, 1989), I predicted that (3) hovering sunbirds would also have significantly short tarsi for their mass. Hovering behavior did not correlate with tarsus length in males nor in females (reject prediction 3). Across all sunbird species, males but not females had significantly short tarsi for their mass compared to what we would expect in geometric similarity. The tendency towards short tarsi in males initially supports the idea that nectar-eating behavior in general, rather than hovering behavior, may drive the need for short tarsi in sunbirds. However, the lack of shortened tarsi in females suggests that alternative selective pressures may be acting on tarsus length in males, rather than nectar-eating behavior. Given that sunbirds frequently obtain nectar from flowers by

perching on the flower stem (Johnson and Brown, 2004; Van der Niet et al., 2015), a longer tarsus may be necessary for foraging.

Female sunbirds increase wing length with elevation

With regards to elevation, I predicted that like hummingbirds, (4) sunbirds will not differ in mass across elevation (Skandalis et al., 2017), and (5) wing length will increase with elevation in hovering sunbirds more than in non-hovering sunbirds (Altshuler and Dudley, 2002; Skandalis et al., 2017). I found that sunbird mass does not correlate with midpoint elevation, maximum elevation, or elevational range (accept prediction 4). I also observed that sunbirds increase wing length with elevation, although the relationship is only significant in females (partially accept prediction 5). This lack of trend between wing length and both hovering behavior and elevation in males further supports the theory that selective pressures outside of aerodynamics drive wing length in males. Male hummingbirds tend to have shorter wings than females (Stiles et al., 2005), potentially as a result of sexual selection. Therefore, wing length in male sunbirds may be driven by pressures of sexual selection in addition to aerodynamics.

Hovering sunbirds do not have relatively long tails

Given the potential need of the tail to assist in pitch and gaze stability (Altshuler et al., 2009; Su et al., 2011; Su et al., 2012; Thomas and Balmford, 1995), I predicted that (6) tail length will scale with positive allometry in hovering sunbirds. I found that hovering behavior did not influence tail length (reject prediction 6). However, the data collected by R. C. K. B. showed that male tails are longer than what would be predicted under geometric similarity, and literature data for females gave a high scaling exponent but was not significantly higher than geometric similarity. Combined, these findings suggest that nectar-eating behavior in all sunbirds, but not hovering species specifically, may require relatively long tails. Literature data on tail length for males showed no dependence on mass, but this may be because this data included measurements of sexually selected elongated tail feathers, which are common in male sunbirds (Skead, 1967).

Nectar-eating selects for some hummingbird-like morphologies in sunbirds

Given that sunbirds tend to have long wings, long tails, and short tarsi relative to their body mass, this work suggests that nectar-eating behavior in general selects for a hummingbird-like morphology. The lack of significance of hovering behavior in analyses for all but one relationship (female wing length) indicates that hovering, particularly asymmetric hovering, does not apply strong selective pressures on sunbird morphology. However, this study defined hovering in a binary fashion. In fact, tendency to hover varies among and within species as certain populations hover frequently and others not at all, perhaps depending on the presence of flowers lacking perches (Geerts and Pauw, 2009; Janeček et al., 2011; Wester, 2013a). Several reports have demonstrated sunbirds frequently obtain nectar from flowers by perching on the flower stem (Johnson, 1996; Johnson and Brown, 2004; Van der Niet et al., 2015) or from the ground (Hobbhahn and Johnson, 2015; Turner and Midgley, 2016). Additionally, some plant species that are frequented by sunbirds have perches to aid in avian nectar-eating and pollination (Anderson et al., 2005). Together, these alternative cases suggest that hovering is a secondary method for sunbirds to obtain nectar, and that selection for morphologies that aid in hovering behavior may be weak. Additionally, presence of hovering behavior is biased by observation, as common and accessible species have more available observations and are therefore more likely

to have been seen hovering. Further study on the morphology of specific populations with different behaviors is required to determine whether hovering behavior alone alters morphology.

My results also indicate strong sexual dimorphism exists in sunbirds. Specifically, males had short tarsi and long tails relative to their body mass while females did not, and female but not male wing length increased with body mass in hovering and high-elevation species. These differences could reflect sexual selection in males, perhaps to increase tail length for displays while reducing mass by shortening tarsus length.

Conclusion

To determine whether asymmetrically hovering birds had adaptations to hovering behavior akin those in symmetrically hovering hummingbirds, I studied morphological trends in the sunbirds, a group including species that do and do not hover. I found that sunbirds are partially convergent on the morphological trends seen in hummingbirds. These changes could be explained by the increased tendency of nectar-eating birds to hover as compared to birds that do not eat primarily nectar. The lack of trend between hovering behavior and morphology suggests that sunbird species employ similar strategies to obtain nectar from flowers, and that those strategies are primarily perching and secondarily hovering. This work broadly suggests that birds do not require specific morphological adaptations to perform asymmetric hovering. Instead, broad trends in morphology may permit birds to hover, and morphological adaptations are not required or do not restrict the appearance of asymmetric hovering. Further work should be done to better quantify hovering ability and determine whether certain morphologies are associated with better asymmetric hovering ability.

Figures

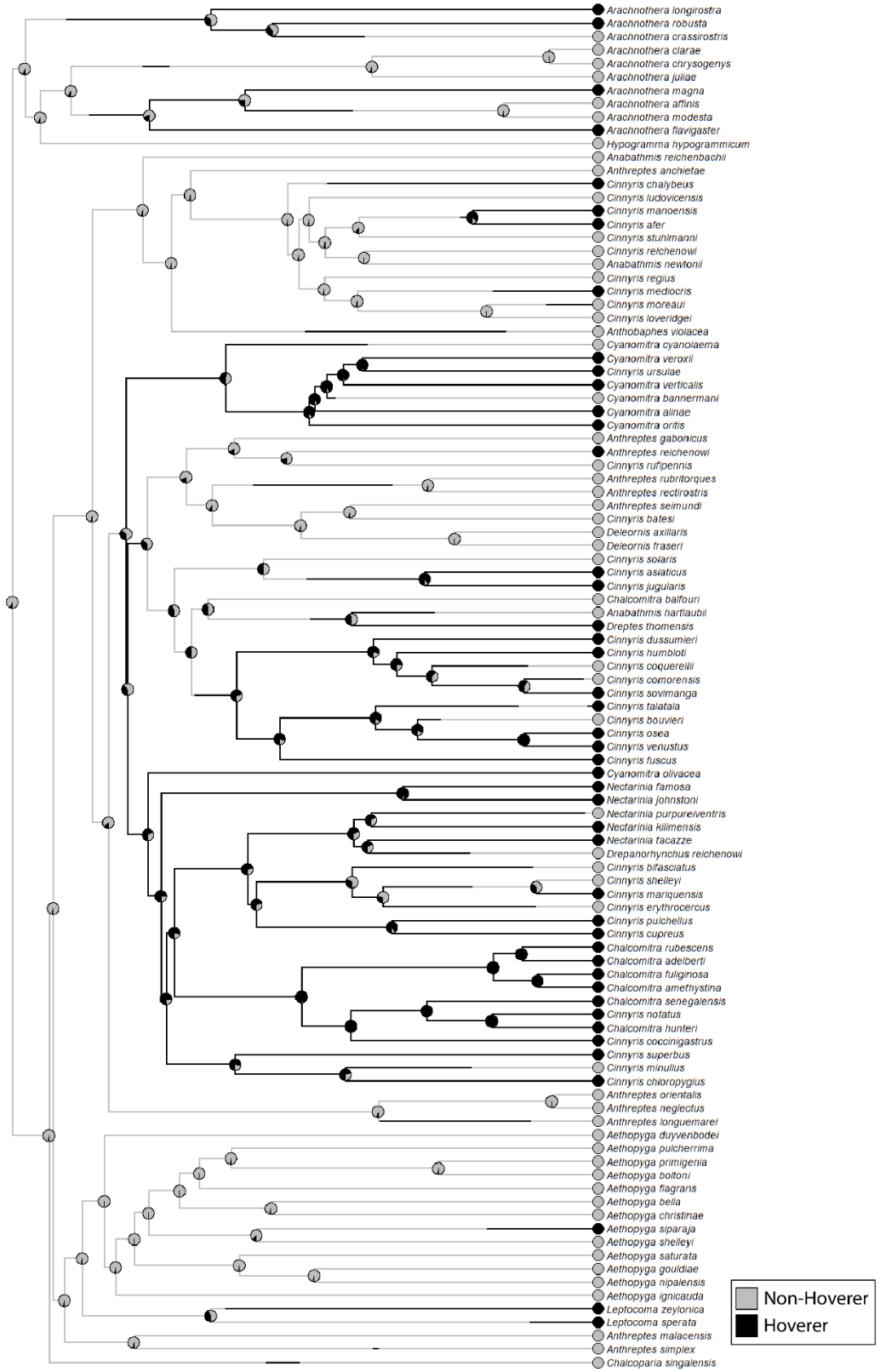

Figure 1-1. Distribution of hovering behavior across the sunbird phylogeny under the all rates equal model of evolution (ΔAICc = 0.00). Branch colors on the underlying tree are from one possible simulation.

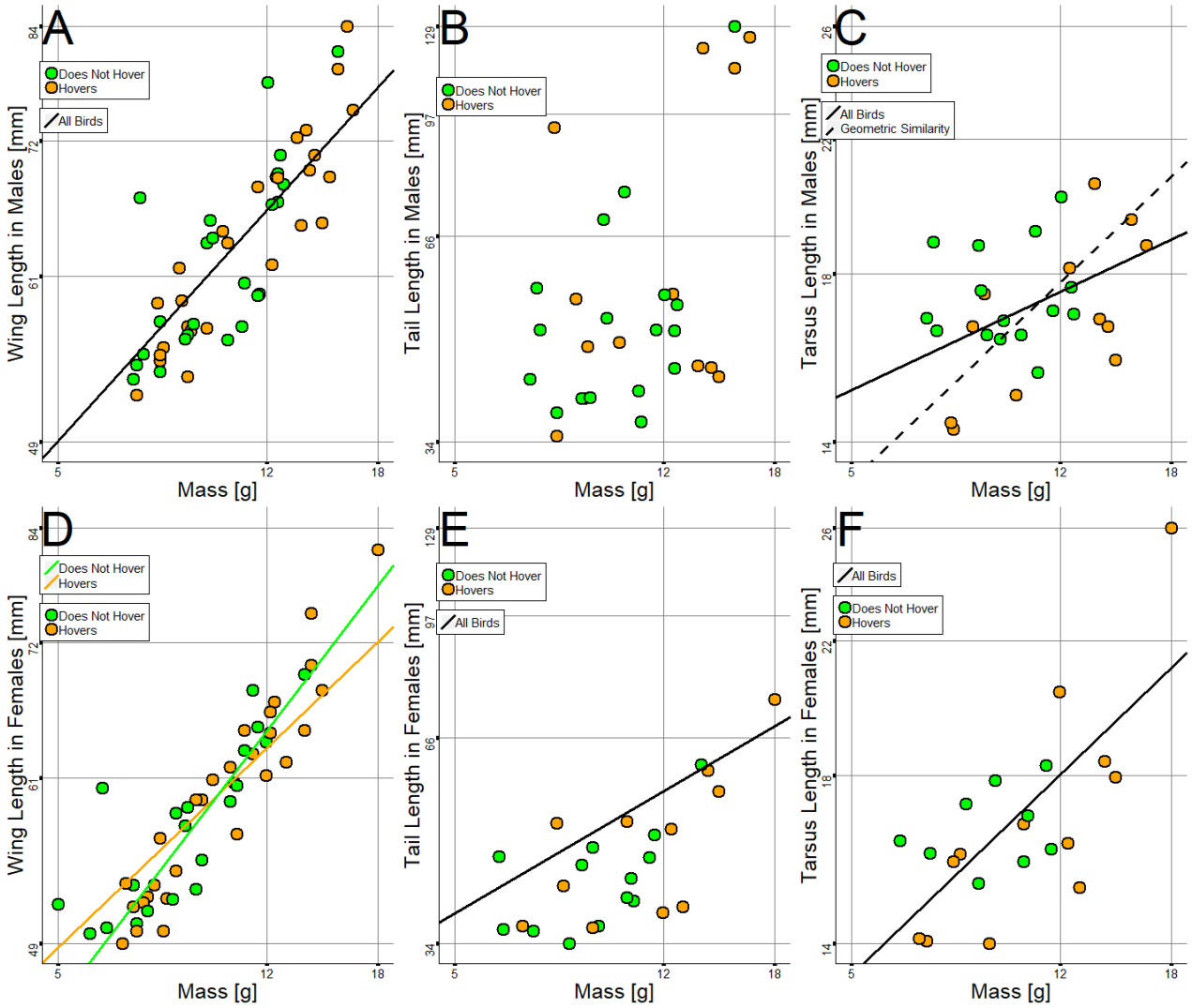

Figure 1-2. Scatterplots of wing (A, D), tail (B, E), and tarsus (C, F) length against mass for males (A, B, C) and females (D, E, F). Light gray dots are for non-hovering species, dark gray lines are for hovering species. Axes are log-transformed. Fit lines are present when the relationship between morphology and mass is significant. Fit lines for wing length were generated from models that included mass and hovering behavior; fit lines for tail and tarsus length were generated from models that used mass only. Dashed lines indicate the prediction under geometric similarity when the predicted slope is significantly different.

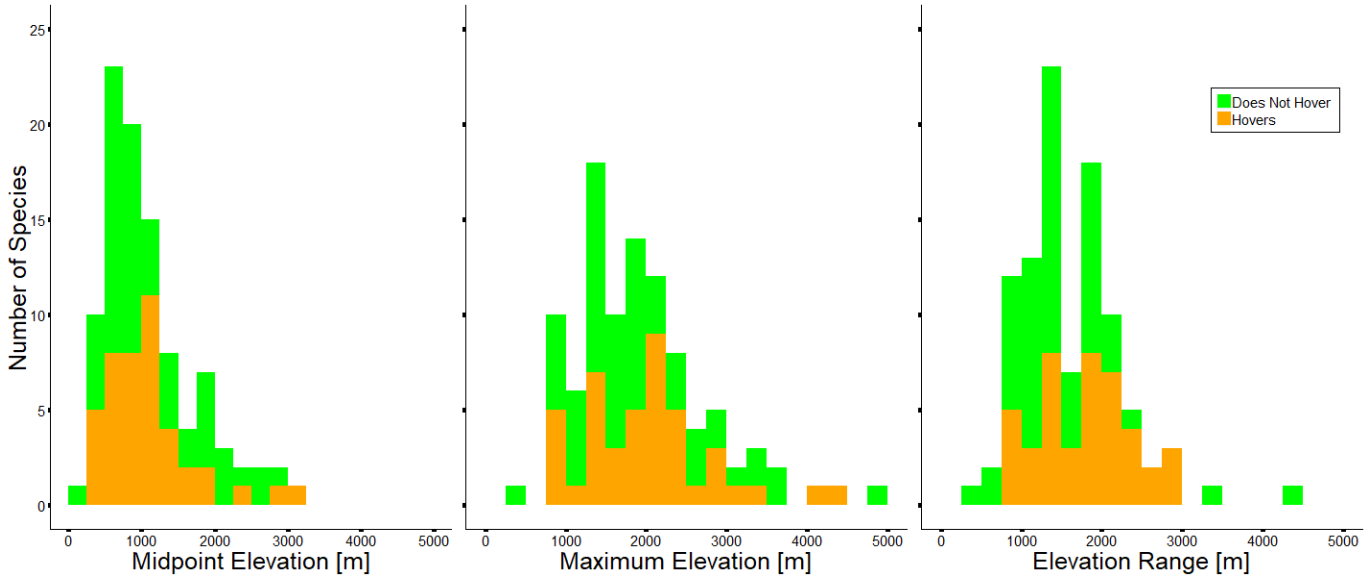

Figure 1-3. Number of sunbird species at average midpoint elevations, maximum elevations, and elevational ranges. Light gray bars are species that do not hover, dark gray bars are species that do hover.

Tables

Table 1-1. Comparison of model fit using ΔAICc. Males (M) and females (F) were tested separately. For each outcome variable, three evolutionary models were tested: the Brownian motion model (BM); the Brownian motion model with Pagel's λ, which modifies the Brownian motion matrix by the parameter λ; and (3) the Ornstein-Uhlenbeck model (OU), which assumes that parameters are moving towards some optimum value. Further, 10 different models using different sets of variables were tested: (1) a model that relates the outcome variable to a constant, assuming none of the variables inform its variance; models in which the outcome variable only depended on mass (2), only depended on hovering behavior (3), or only depended on elevation (4); and additive (Add) and interaction (Int) models for mass with hovering behavior (5 & 6), mass with elevation (7 & 8), and mass, hovering behavior, and elevation. Gray-shaded cells indicate models that fill well (ΔAICc < 7).

							Mass & Hovering		Mass & Elevation		Mass, Hovering, & Elevation	
Character	**Sex**	**Model**	**Constant**	**Mass Only**	**Hover Only**	**Elevation Only**	**Add**	**Int**	**Add**	**Int**	**Add**	**Int**
	M	BM	29.68	2.62	37.07	34.69	10.58	16.46	6.64	12.74	14.33	37.12
		PL	29.76	1.39	33.32	35.42	12.99	19.13	0.00	13.87	6.94	40.77
Wing		OU	32.03	4.94	39.56	37.18	13.04	19.07	9.29	15.55	17.13	40.77
Length	F	BM	41.88	0.00	47.66	48.10	8.46	10.76	4.71	8.51	13.64	34.73
		PL	44.03	1.44	49.72	50.36	10.17	13.02	7.00	10.59	16.06	37.37
		OU	44.25	0.48	50.16	50.60	9.31	12.24	6.93	11.00	16.02	37.93
	M	BM	1.85	3.23	6.22	5.06	8.01	10.89	7.17	10.40	12.89	24.83
		PL	4.01	6.11	7.82	8.02	10.60	13.77	10.86	14.92	16.00	29.96
Tail		OU	0.00	0.40	5.18	3.72	6.04	8.54	5.68	9.98	11.44	28.26
Length	F	BM	4.68	0.91	9.64	9.90	7.16	10.95	6.70	10.57	13.47	31.79
		PL	8.95	0.00	9.62	14.80	6.76	12.46	5.70	11.15	13.03	36.00
		OU	7.48	4.08	12.81	13.06	10.78	15.13	10.32	14.74	17.65	40.23
	M	BM	0.77	0.00	6.94	6.54	5.02	8.92	6.80	12.75	10.57	37.40
		PL	3.23	1.34	9.94	8.89	8.46	12.55	9.99	16.60	14.12	44.70
Tarsus		OU	2.79	3.07	9.61	8.45	8.52	12.57	9.90	16.56	13.98	44.68
Length	F	BM	10.87	0.00	16.67	17.29	7.47	10.16	7.92	12.97	15.77	44.14
		PL	14.49	0.85	20.33	21.66	12.28	13.87	9.25	17.61	21.27	54.06
		OU	13.78	3.36	20.03	20.66	11.40	14.80	11.84	17.53	20.40	55.07

Table 1-2. Coefficients and significance of log-linear morphological relationships with mass as determined using data collected from the literature (Literature) or data measured directly by R. C. K. B. (RCKB). All analyses were modeled using the Ornstein-Uhlenbeck model, although other models of evolution give similar results. The number of species used in each analysis is indicated by *n*. The effect size and its standard error are represented by β. *, **, and *** denote $p < 0.05$, $p < 0.01$, and $p < 0.001$, respectively. The subscript ^{G} indicates that the slope is significantly different from the prediction under geometric similarity.

Character	Sex	Data Source	n	β ±SE			p	
Wing Length	M	Literature	51	0.355	±	0.042	< 0.001	***
		RCKB	11	0.393	±	0.048	< 0.001	***
	F	Literature	49	0.374	±	0.030	< 0.001	***
		RCKB	6	0.353	±	0.043	0.001	**
Tail Length	M	Literature	30	0.459	±	0.245	0.071	
		RCKB	12	0.709	±	0.164	0.002	$**^{G}$
	F	Literature	24	0.423	±	0.124	0.003	**
		RCKB	6	0.474	±	0.413	0.315	
Tarsus Length	M	Literature	27	0.165	±	0.066	0.019	$*^{G}$
		RCKB	11	0.302	±	0.072	0.002	**
	F	Literature	21	0.336	±	0.072	< 0.001	***
		RCKB	4	0.286	±	0.094	0.093	

Table 1-3. Coefficients and significance of log-linear morphology modeled using an interaction model with mass and hovering behavior (~Mass*Hover). Models were performed using the Ornstein-Uhlenbeck model of evolution, although other models of evolution give similar results. The number of species used in each analysis is indicated by *n*. The effect size and its standard error are represented by β. *, **, and *** denote $p < 0.05$, $p < 0.01$, and $p < 0.001$, respectively.

Character	Sex	Data Source	n	Effect	β ±SE			p	
Wing Length	M	Literature	51	Mass	0.359	±	0.063	< 0.001	***
				HoverY	-0.010	±	0.173	0.954	
				Mass:HoverY	-0.001	±	0.076	0.993	
	F	Literature	49	Mass	0.310	±	0.045	< 0.001	***
				HoverY	-0.261	±	0.122	0.038	*
				Mass:HoverY	0.115	±	0.055	0.043	*
Tail Length	M	Literature	30	Mass	0.546	±	0.346	0.127	
				HoverY	0.481	±	1.013	0.639	
				Mass:HoverY	-0.194	±	0.432	0.657	
	F	Literature	24	Mass	0.377	±	0.194	0.067	
				HoverY	-0.088	±	0.515	0.866	
				Mass:HoverY	0.050	±	0.225	0.828	
Tarsus Length	M	Literature	27	Mass	0.077	±	0.109	0.489	
				HoverY	-0.456	±	0.303	0.146	
				Mass:HoverY	0.180	±	0.133	0.189	
	F	Literature	21	Mass	0.137	±	0.150	0.375	
				HoverY	-0.625	±	0.361	0.101	
				Mass:HoverY	0.269	±	0.164	0.120	

Table 1-4. Coefficients and significance of log-linear morphology modeled by an interaction model with mass and elevation (~Mass*Elevation). Models were performed using the Ornstein-Uhlenbeck model of evolution, although other models of evolution give similar results. The number of species used in each analysis is indicated by *n*. The effect size and its standard error are represented by β. *, **, and *** denote $p < 0.05$, $p < 0.01$, and $p < 0.001$, respectively.

Character	**Sex**	**Data Source**	**n**	**Effect**	**β ±SE**			**p**		
Wing Length	M	Literature	39	Mass	0.415	±	0.098	<	0.001	***
				Elevation	0.137	±	0.122		0.268	
				Mass:Elevation	-0.042	±	0.049		0.400	
	F	Literature	38	Mass	0.486	±	0.070	<	0.001	***
				Elevation	0.198	±	0.093		0.040	*
				Mass:Elevation	-0.074	±	0.039		0.070	
Tail Length	M	Literature	23	Mass	0.353	±	0.489		0.480	
				Elevation	-0.015	±	0.738		0.984	
				Mass:Elevation	0.043	±	0.299		0.889	
	F	Literature	20	Mass	0.753	±	0.284		0.018	*
				Elevation	0.526	±	0.362		0.166	
				Mass:Elevation	-0.199	±	0.154		0.215	
Tarsus Length	M	Literature	21	Mass	0.107	±	0.181		0.562	
				Elevation	-0.075	±	0.228		0.748	
				Mass:Elevation	0.049	±	0.095		0.615	
	F	Literature	18	Mass	0.657	±	0.191		0.004	**
				Elevation	0.485	±	0.283		0.109	
				Mass:Elevation	-0.190	±	0.117		0.125	

Chapter 2.Influence of Migratory Behavior on Bone Morphology in the Dark-Eyed Junco (*Junco hyemalis*)

Introduction

Climate change alters the latitudinal and elevational distribution of birds (Tingley et al., 2009; Tingley et al., 2012). These movements may also alter migratory behavior, potentially reducing migratory distance or ablating migratory behavior altogether. Changes to migratory behavior will influence flight behavior, and ultimately morphology. To understand the potential influences of altered migratory behavior on morphology, I studied how morphology differs across the Dark-Eyed Junco (*Junco hyemalis*), a species whose subspecies differ in their migratory status (e.g. whether they are a permanent resident or a migrant).

Migratory behavior in birds requires massive increases in energy expenditure due to increased time spent each day in locomotion (Wikelski et al., 2003). To prepare for this challenge, some migratory birds increase body mass (Wolfson, 1945), reduce the size of digestive organs (Battley and Piersmazs, 1997; Piersma and Gill, 1998), and increase the mass of muscles related to flight (*M. pectoralis* and *M. supracoracoideus*) but not the mass of leg muscles (Battley and Piersmazs, 1997; Lindström et al., 2000; Marsh, 1984). During migration, birds appear to lose fat stores but also muscle mass (Biebach, 1998). These rapid changes in body and muscle mass may lead to changes in the magnitude and rate of load applied to the bone, potentially resulting in drastic increases or decreases in bone mass (Kodama et al., 2000; Morey-Holton and Globus, 1998; Shipov et al., 2010; Tromp et al., 2006) or even fatigue fractures (Orava et al., 1978).

The exact endocrine mechanisms by which these pre-migratory changes occur has been reviewed elsewhere (Wingfield et al., 1990). Generally, testosterone and thyroid hormone must be present for pre-migratory hyperphagia and restlessness to occur, and pre-migratory changes themselves may be connected to increases in corticosterone and prolactin secretion resulting from changes in day length (Holberton et al., 2008; Meier et al., 1965; Wingfield et al., 1990).

However, while the nature and underlying mechanisms of pre-migratory changes in digestive organs, muscles, and fat prior to migration have been well studied, a knowledge of whether bone changes prior to or during migratory behavior is lacking. This is especially important because the simultaneous increase in mass and number of loads of bone during migratory flight could lead to an increased risk of fatigue fracture. Specifically, massive increases in body mass could increase strain and strain rate on bone, resulting in increased microdamage (Chamay, 1970; Schaffler et al., 1989) and an increased risk of fracture incidence (Reilly and Currey, 2000).

Additionally, we might expect alterations in bone morphology to occur as a direct result of the other changes that occur prior to migration. For example, an increase in body mass could cause an increase in overall stress on bones, which would lead to an increase in bone mass throughout the body (Rubin and Lanyon, 1985). Additionally, bone mass has been associated with muscle mass and muscle strength (Burr, 1997). Given that the muscles involved in flight but not leg muscles hypertrophy prior to migration (Battley and Piersmazs, 1997; Marsh, 1984), there might be an increase in bone mass or bone strength in wing bones but not leg bones.

The potential influences of prolactin bone are more complex. Prolactin seems to increase bone turnover in mice and rats (Krishnamra and Seemoung, 2011; Lotinun et al., 2003) and may lead to reduced bone formation and development in developing rats (Coss et al., 2017). Additionally, elevated prolactin levels have been observed in schizophrenic patients receiving certain antipsychotic medications, and this has been associated with reduced bone mineral density and bone loss (Meaney et al., 2004). Increased prolactin levels in pre-migratory birds may therefore lead to systemic reductions in bone mineral density and bone loss.

I therefore sought to determine the influence of migratory behavior on bone morphology in birds. To do this, I used the Dark-Eyed Junco (*Junco hyemalis*), a species that is widespread across North America and includes subspecies that do not migrate (e.g. "residents*", J. h. carolinensis, J. h. pontilis*) and species that do migrate (e.g. "migrants", *J. h. hyemalis, J. h. montanus, J. h. aikeni*). To determine whether systemic effects such as increased body mass or alterations in hormones influence bone mass or bone morphology, I compared two compartments within each bone: the strut-like region of trabecular bone in the metaphysis (proximal and distal ends of the bone), and the compact cortical bone in the diaphysis (the midshaft or middle of the bone) in resident and migrant birds. To tease apart the influences of increased body mass versus increased muscle mass in migratory birds, I compared bone volume and morphology in a bone primarily involved in flight (the humerus) with one not involved in the flight (the femur) in residents and migrants.

Methods

Specimens

In order to assess the influence of migratory behavior on bone independent of mass and evolutionary history, several subspecies were used (Figure 2-1). Within the Slate-Colored (Hyemalis) group, *Junco hyemalis hyemalis* represented the migrant form, while *J. h. carolinensis* represented the resident form. Within the Oregon (Oreganus) group, *J. h. montanus* represented the migrant form, while *J. h. pontilis* represented the resident form. The White-Winged Junco, *J. h. aikeni* was used as an intermediate, both phylogenetically and because it is a short-distance migrant (Aleixandre et al., 2016).

Skeletal samples were loaned from the American Museum of Natural History (*J. h. hyemalis* n = 18, *J. h. aikeni* n = 20, *J. h. carolinensis* n = 20, *J. h. montanus* n = 20, *J. h. pontilis* n = 9). Only male specimens were used because female specimens frequently contained medullary bone, a bony tissue formed prior to egg-laying which greatly alters cross-sectional skeletal morphology (Dacke et al., 2015). To ensure that only adults were taken, specimens labelled as 'hatch year' or those with less than 100% skull ossification were removed. Specimens from migratory subspecies would ideally be taken immediately after arriving on their breeding grounds to reduce the influence of post-migratory changes (e.g. reduction in body fat, testes growth) on bone morphology. This time varies by subspecies, sex, and age (Chandler and Mulvihill, 1990; Nolan and Ketterson, 1990). In practice, specimen availability dictated which specimens were taken. Where more than 20 samples were available, samples were randomly chosen to span the available sampling locations.

For each specimen, one humerus and one femur was scanned. The left bone was used unless it was broken, missing, or still attached to the skeleton, in which case the right bone was used. To

keep scanning conditions similar across all samples, bones were placed in a 3D-printed sample holder that held four samples at a time (a humerus and a femur from two birds), and then scanned in air. Scanning in air increases x-ray beam attenuation compared with scanning in other media (saline, ethanol) and thus influences measured density (Bouxsein et al., 2010; Nazarian et al., 2008). The densities reported here are therefore for comparative purposes only and should not be used as true measures of density in *J. hyemalis* bone.

Micro-computed tomography scanning

Bone morphology and microarchitecture were assessing using a high-resolution micro-CT scanner (μCT 35, Scanco Medical, Brüttisellen, Switzerland) at an x-ray energy of 70 kVP, integration time of 300 ms, and an isotropic voxel size of 6 μm.

Cortical bone morphology was assessed using a 0.6 mm long region centered around the center of the bone midshaft. To assess trabecular (cancellous) bone morphology, 0.6 mm long endosteal regions were defined. The region was kept 0.036 mm away from the endosteal surface of the cortex to ensure that no cortical bone was included in the analysis. In the humerus, the region was in the proximo-caudal portion of the bone, just distal to the opening of the fossa pneumotricipitalis. In the femur, the region was just proximal to the portion of the scan in which both femoral condyles were present. These regions were outlined using semi-automatic region-drawing scripts, then a threshold of 540 mmHg/cm^3 was applied to separate bone from air.

To determine bone morphological properties, a Scanco script employing distance transformation methods was used. Cortical morphological properties included bone volume fraction (Vol. Frac, (%)), tissue mineral density (TMD, mgHA/cm^3), bone volume (CtBV (mm^3)), cortical thickness (CtTh (mm)), cortical diameter (Diam (mm)), polar moment of inertia (pMOI (mm^4)), maximum moment of inertia (I_{max} (mm^4)), and minimum moment of inertia (I_{min} (mm^4)). Trabecular morphological properties included bone volume fraction (Vol. Frac., (%)), bone volume (TbBV (mm^3)), trabecular number (TbN (1/mm)), trabecular thickness (TbTh (mm)), and structural model index (SMI).

Whole bone stiffness, that is, whole bone resistance to loading, is proportional to material and geometric properties. Bird bones experience many forms of loading, but the largest ones are bending and torsion (Biewener and Dial, 1995). Resistance to bending is proportional to *EI*, where *E* is the Young's modulus, or the stiffness of the material in bending; and *I* is the second moment of area in bending, or the geometric arrangement of material in the cross section. Resistance to torsion is *GJ*, where *G* is the shear modulus, or the stiffness of the material in torsion; and *J* is the second moment of area in torsion, usually equivalent to pMOI. The stiffness moduli *E* and *G* are thought to depend primarily on mineral density in bone (Guo, 2001; Launey et al., 2010). Since mineral density was similar in all of the bones used here, I assume that whole bone stiffness will primarily vary with the geometric properties of *I* and *J* (pMOI). For this reason, I hereafter refer use the terms "geometric bending stiffness" synonymously with I_{max} and I_{min}, and "geometric torsional stiffness" synonymously pMOI.

Statistical analyses

Linear mixed effects models were implemented in RStudio (RStudio Team, 2015) using the *lme* function in the *nlme* package (Pinheiro et al., 2019). For bone morphology analyses in which the

outcome variable had units of length, mass and the outcome were log-transformed prior to analyses.

First, to determine which variables significantly explain bone morphology, several models were tested that included one or more of bird mass, subspecies, migratory status (resident or migrant), altitude, and day of the year (as an integer). Then, the best model was identified using the second order Akaike Information Criterion (ΔAICc). This method determines whether each additional term in a model significantly improves fit, and also takes sample size into account (Burnham and Anderson, 2002). A model with a score of less than 7 was considered to be a good fit.

Second, because was interested primarily in the influence of mass and migratory status on bone morphology, I pooled data on residential and migratory individuals from all subspecies. Then, I modeled each morphological variable as an additive function of mass and migratory status. Altitude and day of the year were included as random effects. A p-value cutoff of 0.05 was used to determine whether each term explained a significant portion of that morphological variable.

Results

Variables contributing to model fit

Model fits based on ΔAICc scores are shown in (Table 2-1). Altitude and day of the year did not significantly explain any aspects of bone morphology, except for femur trabecular thickness, where altitude was an acceptable model.

Bone length. Both humerus and femur length in males were best explained either by a model that included just subspecies, or an additive model with mass and subspecies.

Trabecular morphology. A constant was the best model for most trabecular morphology parameters. In the humerus, migratory status was also a good model for trabecular volume fraction, trabecular number, and SMI. Mass was a good model for humeral trabecular volume and number. In the femur, migratory status was a good model for trabecular volume fraction, trabecular number, trabecular thickness, and SMI; subspecies was also a good model for explaining trabecular volume and SMI. For both the humerus and the femur, trabecular connective density was best explained by a model including additive and interaction terms for mass and subspecies.

Cortical morphology. A model including mass or an additive model with mass and migratory status were the best models for most cortical morphology parameters. However, cortical bone volume fraction differed as the best fit models included either a constant or subspecies. Cortical thickness could also be modeled by a constant for both the humerus and femur. Cortical bone volume differed between the humerus and femur: in the humerus, a model with mass was the only good fit for cortical bone volume, while in the femur, an additive model with mass and migratory status was the only good fit. In the humerus, a model that also included the interaction of mass and migratory status was a good fit for pMOI and I_{max}.

Influence of mass and migratory status on bone morphology
All morphological variables were modeled as a function of mass and migratory status with altitude and day of the year as random effects. See Table 2-2 for the significance and effect size of all morphological variables.

Bone length. Mass was a significant explanatory variable for bone length in both the humerus and femur of male birds (Figure 2-2). In the femur, migratory status was also significant: migrants had significantly shorter femora than residents (-0.017 ± 0.008, p=0.049).

Trabecular morphology. Volume fraction did not depend on mass or migratory status in resident or migrant male birds. Bone volume was explained by mass for both the humerus and femur, but not by migratory status (Figure 2-3). Neither mass nor migratory status could explain any other trabecular morphology in the humerus. However, in the femur, trabecular thickness was decreased in migrants (-0.091 ± 0.039, p=0.033). Migrants also had higher trabecular connective density than residents (0.399 ± 0.185, p=0.047).

Cortical morphology. In both the humerus and femur of male birds, cortical volume fraction was not significantly associated with mass but was significantly lower in migrants (humerus: -0.025 ± 0.007, p=0.002; femur: -0.022 ± 0.006, p=0.001). Tissue mineral density also did not depend on mass but was lower in migratory femora (-88.5 ± 36.9, p=0.030). All other cortical morphologies (volume, thickness, diameter, pMOI, I_{max}, I_{min}) increased significantly with mass in both the humerus and femur (Figure 2-4). Additionally, migrant humeri had the same bone volume as resident humeri (p=0.524), but migrant humeri were significantly thinner (-0.050 ± 0.018, p=0.013) and wider (0.025 ± 0.009, p=0.009). These changes did not result in any changes in pMOI, I_{max}, or I_{min} (p=0.185, p=0.187, p=0.184, respectively). Migrant femora had lower bone volume (-0.087 ± 0.022, p=0.001), and their femora were significantly thinner (-0.090 ± 0.018, p<0.001), but diameter was not different (p=0.382). This resulted in lower pMOI (-0.103 ± 0.043, p=0.032), I_{max} (-0.106 ± 0.044, p=0.030), and I_{min} (-0.098 ± 0.045, p=0.047).

Discussion
To determine whether and how migratory behavior alters bone mass and morphology, I compared male representatives of resident (*J. h. carolinensis*, *J. h. pontilis*) and migrant (*J. h. hyemalis*, *J. h. montanus*, *J. h. aikeni*) subspecies of the Dark-Eyed Junco (*Junco hyemalis*). I looked at a bone primarily involved in flight (the humerus) as well as one not involved in flight (the femur) and at both trabecular and cortical compartments of bone to tease apart the influences of systemic pre-migratory hormones, pre-migratory hyperphagia, and increased mass of muscles related to flight on bone morphology. I found that migratory birds had humeri with lower bone volume fraction because they were significantly wider and thinner, but that these changes did not alter geometric bending or torsional stiffness. In contrast, migrant femora had lower bone volume fraction due to significantly less cortical bone, a thinner cortex, and lower tissue mineral density, resulting in lower geometric bending and torsional stiffness. Migrants also had lower trabecular bone thickness in the femur. Below, I broadly discuss the potential mechanisms driving these differences. I first discuss potential endocrine mechanisms that may result in these changes over an individual's lifetime. Then, I discuss how differences between behaviors of migrants and residents may result in morphology differences over evolutionary time. Finally, I

discuss other potential explanations for the morphological trends seen here, including time of collection and subspecies differences.

Physiology and morphology in migratory juncos

Bone volume decreases in the femoral cortical region but not in the trabecular region. This suggests that pre-migratory increases in hormones or in body mass may not cause systemic increases in bone mass. However, studies have shown that the primary effect of prolactin is to increase calcium resorption and bone turnover (Coss et al., 2017; Krishnamra and Seemoung, 2011; Lotinun et al., 2003). I did observe a significant decrease in femoral cortical tissue mineral density in migratory birds, but this effect was not observed in the humerus. This suggests that prolactin may cause calcium resorption, but that the effect is modulated by other factors.

The differences in the influence of migratory behavior on humerus and femur cortical morphology suggest that large increases in body mass during migration do not correlate with bone morphology. Although the loads per day during migration are presumably higher in the humerus than in the femur, the femur does experience loading during stopovers. A small number of load applications per day are required in order to maintain a given bone mass, beyond which additional load applications do not greatly increase bone mass (Rubin and Lanyon, 1984). Therefore, an increased body mass should theoretically cause similar increases in the humerus and femur. Given that femur but not humerus bone volume is decreased in migratory birds, factors other than body mass may contribute to bone volume. For example, increased muscle mass in the migrant pectoralis but not in the leg muscles may be correlated with the differences in cortical bone morphology (Battley and Piersmazs, 1997; Marsh, 1984). However, such increases would tend to an increase bone mass in the humerus but not in the femur. In contrast, I see similar bone mass in the humerus in residents and migrants, but decreased bone mass in migratory femora.

An alternate explanation could be a combination of the two influences: the pre-migratory spike in prolactin may initially decrease bone mass and tissue mineral density in both the femur and humerus. However, the increased pectoral muscle mass in migrants may then increase strains on the humerus, leading to recovery of bone mass or prevention of bone loss. In contrast, a lack of increase in muscle mass in the femur may cause it to experience only the losses from prolactin. It has also been shown that migratory behavior itself leads to the loss of muscle mass in both the flight apparatus and in the legs (Piersma, Gudmundsson and Lilliendahl, 1999; Lindström et al., 2000; Engel, Biebach and Visser, 2006). Given that muscle mass increases in the flight apparatus but not in the legs prior to migration (Marsh, 1984; Battley and Piersmazs, 1997), the losses in muscle mass during migration could result in a cumulative loss in muscle mass in the legs but not in the flight apparatus. Since loss of muscle mass is associated with loss of bone mass (Burr, 1997), this could also result in the overall loss of bone mass at the femur.

Yet another explanation for the lack of difference between migratory and resident birds in geometric stiffness of the humerus may be that the humerus is under similar forces regardless of whether a bird migrates or not. In order to tolerate changes in climate during the winter, resident birds are known to acclimatize primarily by shivering (Dawson et al., 1983). Although not as metabolically expensive as flight, shivering does increase basal metabolic rate during the winter, and as such resident birds build up energy stores prior to the winter season much like migrants

do prior to migration. Additionally, the muscles primarily used in shivering thermogenesis are the flight muscles. Therefore, the lack of difference in humerus morphology between residents and migrants may be in part because both groups apply similar strains on their humeri during the winter, resulting in similar humerus morphology.

Evolutionary differences between migrant and resident juncos

The birds used in this study were collected during the months of breeding (May through July), rather than directly before or during migration (March through May) (Figure 2-5) (Nolan, Jr. et al., 2002). Therefore, differences in bone morphology as a direct result of pre-migratory and migratory behavior may have been reversed by the time specimens were collected and thus not present in these specimens. For example, the migratory subspecies *J. h. hyemalis* has been shown to have shorter, more pointed wings for a given body mass than its close relative, the resident subspecies *J. h. carolinensis* (Mulvihill and Chandler, 1991). This may alter the torsional forces and lead to the thinner, wider humeri observed in migrants in this study.

Migratory birds may have stronger selective pressures to reduce bone mass due to the expense of transporting it during long-distance migration. Specifically, the selection to reduce overall mass may be stronger than selection to maintain geometric stiffness and strength in the femur, ultimately resulting in the observed trend of lower bone mass in migratory femora. Work on alligators has shown that safety factor can differ between different limbs in the same animal due to variations in load or high safety factors overall (Blob et al., 2014). In migratory birds, reduced loading on the femur during migration and high safety factors in all bones may reduce selection for high geometric stiffness and increase selection for reduced mass.

Finally, although the endocrine mechanisms discussed above may not change the morphology of an individual during each migration, they may still underlie the differences between residents and migrants. That is, differences in the overall endocrine environment of migrants versus residents over their lifetimes may gradually cause the changes shown here in migratory birds, thereby differentiating them from residents.

Regardless of the mechanisms driving differences in morphology between resident and migrant *J. hyemalis* exist, the finding that migrant femora are less stiff than resident femora suggests that selective pressures may be constraining bone mass in migrants. If climate change reduces migratory behavior, these pressures may be lifted, allowing migrants to have stiffer and heavier femora. It is unclear whether this would be a benefit, as stiffer femora may be more prone to fracture due to reduced toughness (Schaffler et al., 1995).

Morphological differences across subspecies

Several subspecies of *J. hyemalis* were used in this study, each of which represents a distinct lineage (Aleixandre et al., 2016) with distinct habits. My model exploration suggested that only bone length and trabecular connective density were best explained by subspecies differences. This suggests that while subspecies may differ in bone size, other bone morphological parameters are better explained by mass and/or migratory status.

Additionally, the individuals used in this study vary in the location, latitude (Figure 2-1), and altitude (Figure 2-6) at which they were captured. Increased latitude is known to increase body

mass in *J. hyemalis* (Nolan, Jr. and Ketterson, 1983). Given that migrants were broadly taken from higher latitudes, my results for migratory status may be confounded with results for higher latitude.

Subspecies also differ broadly in behavior (Nolan, Jr. et al., 2002), e.g. time spent foraging on the ground versus in trees and bushes, food preferences, and timing of breeding. These differences, as well as evolutionary drift, may explain differences in bone morphology. Further work being performed to determine the extent to which bone morphology can be modeled by subspecies rather than migratory status.

Other factors driving bone morphology

Day of the year did not significantly improve model fit, as determined with ΔAICc, for any aspect of bone morphology. This suggests that time of year does not contribute significantly to bone morphology, at least compared with mass and migratory behavior. However, birds used in this study were all taken during the breeding season, and therefore any differences that occur during the year due to molt, migratory behavior itself, wintering, or other behaviors are not included in the day of the year variable. Indeed, bone density has been shown to go down in poultry during molt (Hester et al., 2004). In order to determine whether bird bone morphology changes significantly over the course of the year, a study including birds from different times of year is required.

Model fit also did not improve with the inclusion of altitude for any variable except femur trabecular thickness. Increased altitude reduces air density and thus reduces the lift that can be produced under the same flight kinematics. Recent work in hummingbirds has suggested that the primary mechanism by which birds overcome this disparity is by increasing wing area, rather than by changing wing velocity or other kinematic parameters (Skandalis et al., 2017). As such, we might not except altitude to significantly influence bone morphology. However, birds used in this study were not collected with the goal of exploring variation across elevations, and sampling is therefore concentrated on specific elevations at which collecting trips occurred (Figure 2-6). Further, expect for *J. h. montanus*, subspecies tend to be distributed at certain elevations, and this metric may therefore be confounded with subspecies.

Future work

The data presented here gives initial support to the potential role of pre-migratory changes in influencing bone morphology via increases in prolactin, increase in whole body mass, and increases in muscle mass. However, this study compared subspecies of *J. hyemalis* collected during breeding. To better determine the exact influence of pre-migratory hormones and changes in body and muscle mass, future studies should compare migratory juncos that are allowed to migrate or fly in a wind tunnel with those that are prevented from flying, or perform *in vivo* micro-computed tomography scanning before, during and after migration to elucidate changes.

Conclusion

To understand the influences of migratory behavior on bone morphology in birds, I compared trabecular and cortical morphology in the femur and humerus of resident and migrant Dark-Eyed Juncos (*Junco hyemalis*). I found that migrant humeri are wider and thinner than resident humeri, but that they do not differ in the amount of bone or in whole bone geometric stiffness. In

contrast, migrant femora had less bone due to a thinner cortex, resulting in bone that had lower geometric stiffness overall. I propose that these differences are due to two combined changes that occur in the pre-migratory period: increased prolactin secretion, and increased mass of the muscles involved in flight but not in the leg muscles. Prolactin increases calcium resorption, which is nullified by increased load by larger flight muscle mass in the humerus but not in the femur. Alternatively, broad evolutionary differences between residents and migrants, including differences in the endocrine environment, may drive morphological variation. Regardless, these findings suggest that migratory birds may be under selective pressures that reduce their bone mass. These pressures would be lifted if migratory distance was reduced during climate change, potentially altering bone morphology. Further study should compare bone morphology in a single population of migratory birds that is allowed and prevented from flying in order to determine the exact influences of pre-migratory and migratory behavior on bone, and thus the potential changes that might result from reduced migratory behavior under climate change.

Figures

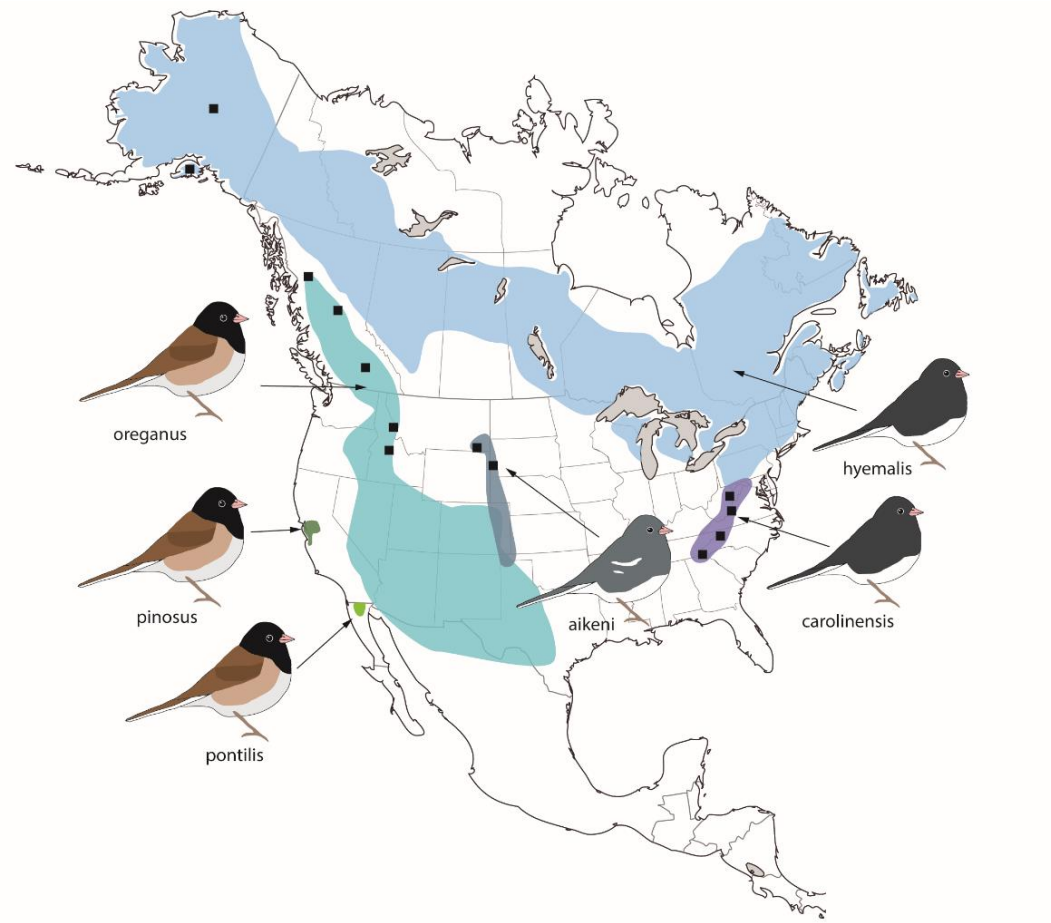

Figure 2-1. Distribution of *Junco hyemalis* subspecies used. Black dots represent locations from which samples were taken. Figure modified with permission from (Aleixandre et al., 2016).

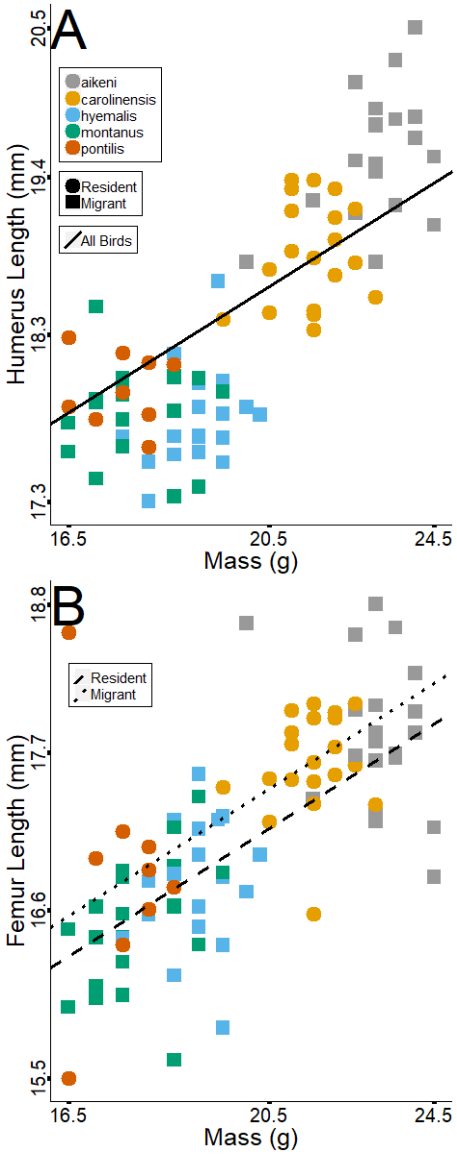

Figure 2-2. Junco humerus (A) and femur (B) length as a function of mass in residents (circles) and migrants (squares) of various species (colors). Axes are log-transformed, values are actual, and each dot represents one individual. The solid line in A indicates that humerus length is significantly explained by mass ($p<0.001$), but not by migratory status ($p=0.286$). The two lines in B indicate that femur length is significantly explained by mass ($p<0.001$) and migratory status ($p=0.021$).

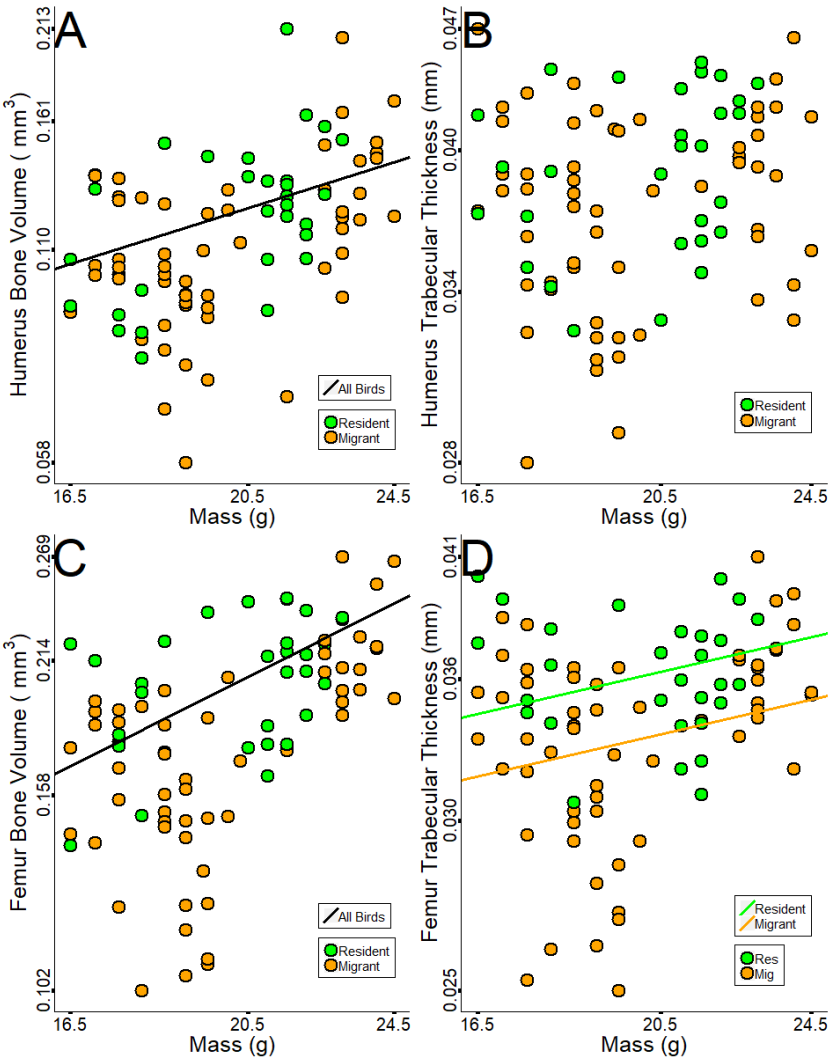

Figure 2-3. Trabecular bone morphology in the humerus (A, B) and femur (C, D). Resident birds are in green, migrant birds in orange. Axes are log-transformed, values are actual, and each dot represents one individual. A black line indicates a significant relationship between mass and the morphological measurement, but no relationship of the morphological measurement with migratory status. Green and orange lines indicate significant differences between residents and migrants. Bot humerus and femur bone volume increased with mass ($p_{humerus}$=0.009, p_{femur}=0.002), but was not influenced by migratory status ($p_{humerus}$=0.237, p_{femur}=0.110). Trabecular thickness does not depend on mass (p=0.889) or on migratory status (p=0.123) in the humerus. In the femur, trabecular thickness is not influenced by mass (p=0.598) but is lower in migrants (p=0.033).

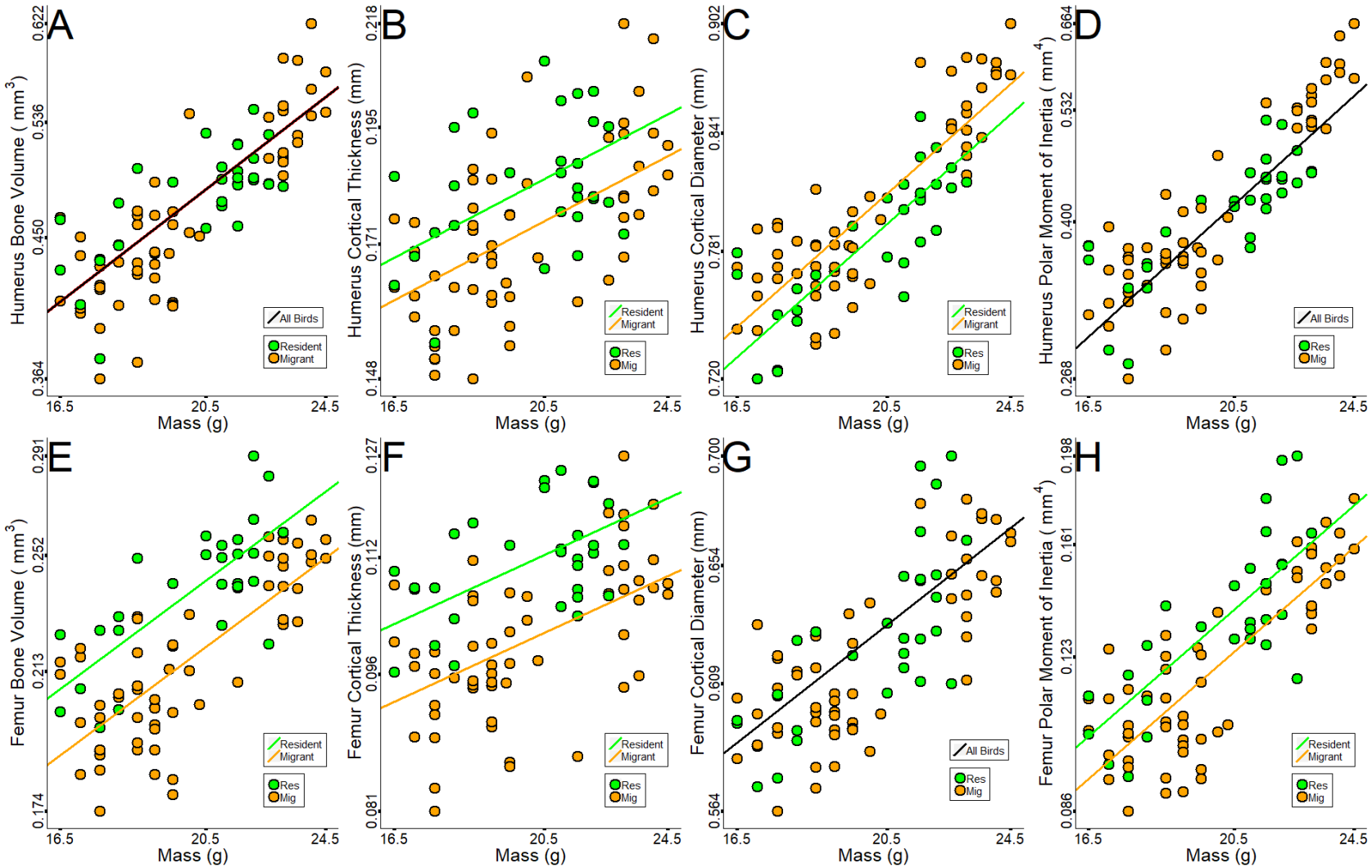

Figure 2-4. Cortical bone morphology in the humerus (A, B, C, D) and femur (E, F, G, H). See Fig. 3 caption for other figure notes. Cortical volume, thickness, diameter, and torsional stiffness (pMOI) depend on mass in both the humerus and femur ($p<0.001$). In the humerus, migrants have a thinner ($p=0.013$) but wider ($p=0.016$) cortex but are not different in pMOI ($p=0.185$). In the femur, migrants have significantly less bone in the cortex ($p=0.001$), lower cortical thickness ($p<0.001$), and lower pMOI ($p=0.032$), but do not differ in cortical diameter ($p=0.382$).

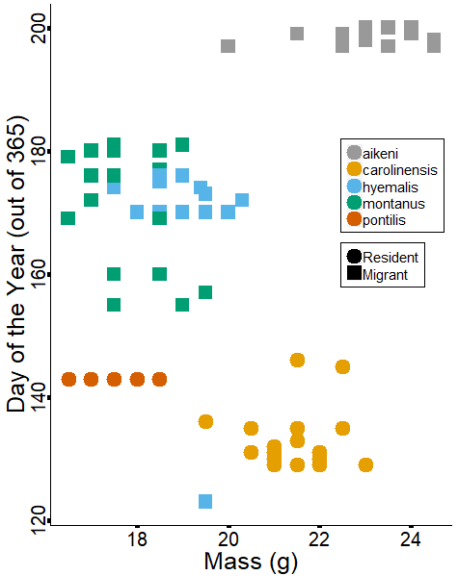

Figure 2-5. Day of the year at which birds from various subspecies (colors) were collected. Birds were collected from early May (121 = May 1st) through mid-July (200 = July 19). Each dot represents one individual.

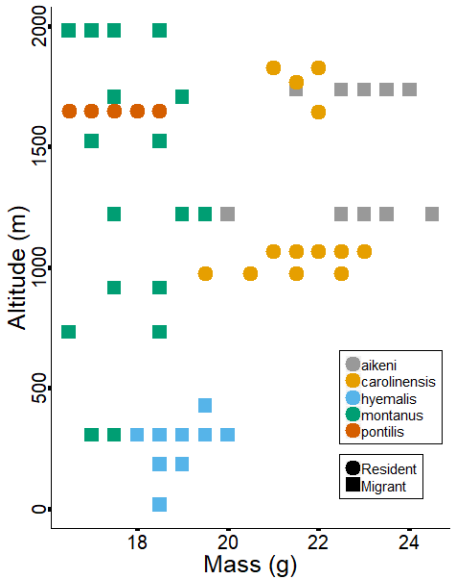

Figure 2-6. Altitude at the subspecies (colors) were collected as a function of their mass. Individuals collected on the same trip tended to be collected at specific altitudes. Axes are log-transformed, values are actual, and each dot represents one individual.

Tables

Table 2-1. Comparison of model fit using ΔAICc. For each morphological measurement, 19 models were tested that combined mass, migratory status (Stat, Resident vs. Migrant), subspecies (Subspp), day, and altitude (Alti). Subspecies and migratory status result in a singularity in model fitting, and therefore only one could be used in any given model. Models with ΔAICc < 7 have shaded cells. Conn. Dens. = connective density; F = femur; H = humerus; Imax = maximum second moment of area; Imin = minimum second moment of area; pMOI = polar moment of inertia; SMI = Structural Model Index; Vol. Frac. = volume fraction.

			~1	~Mass	~Stat	~Subspp	~Day	~Alti	~Mass* Subspp	~Mass+ Subspp	~Mass* Stat	~Mass+ Stat	~Mass* Day	~Mass* Alti	~Stat* Day	~Stat* Altit	~Day* Alti	~Mass* Stat*Day	~Mass* Stat*Alti	~Status*	~Mass* Stat* Alti*Day
	H	**Length**	107	23	111	0	112	113	19	3	27	27	43	40	50	123	135	41	72	111	186
	F	**Length**	42	7	43	0	53	56	15	6	12	7	29	41	33	71	88	49	77	97	196
Trabecular Morphology	**Humerus**	**Vol. Frac.**	0	11	6	32	17	25	85	43	30	17	46	62	38	53	72	92	128	138	292
		Volume	6	0	14	18	24	28	66	29	20	8	36	49	34	55	76	77	114	127	271
		Number	0	6	5	18	13	20	39	23	19	11	34	47	27	42	58	54	96	109	215
		Thickness	0	15	11	28	21	17	95	43	41	26	59	63	45	49	69	110	137	148	332
		SMI	0	9	4	16	12	19	39	19	21	13	35	50	26	41	54	60	92	106	214
		Conn. Dens.	62	62	58	35	67	62	0	33	56	58	72	71	60	67	82	52	75	98	130
	Femur	**Vol. Frac.**	0	11	6	8	19	12	63	18	27	17	42	52	32	44	62	81	118	129	276
		Volume	24	12	28	0	42	30	47	10	24	14	41	45	31	54	76	65	103	124	252
		Number	0	9	3	17	11	17	42	23	19	12	34	46	22	38	53	57	92	101	218
		Thickness	0	14	4	13	21	6	80	29	32	18	52	53	32	35	58	97	122	137	308
		SMI	5	14	6	0	19	8	21	6	22	15	41	39	25	30	47	60	81	95	206
		Conn. Dens.	133	131	122	57	135	115	0	50	117	120	137	123	115	110	130	88	112	132	134
Cortical Morphology	**Humerus**	**Vol. Frac.**	1	15	0	29	11	25	74	41	25	14	42	64	31	46	64	84	117	130	278
		Volume	59	0	68	22	70	76	64	27	19	10	35	44	40	99	112	70	105	128	267
		Thickness	5	0	12	23	24	27	77	36	18	5	36	52	27	56	76	81	114	130	288
		Diameter	68	0	73	12	63	87	54	16	10	1	19	46	36	104	108	61	103	122	261
		pMOI	86	0	92	11	84	102	41	8	7	5	17	40	43	119	124	50	93	124	243
		Imax	81	0	88	13	80	98	48	13	7	7	17	44	43	119	123	56	98	132	258
		Imin	83	0	90	17	82	100	59	17	15	6	24	43	47	120	125	62	105	130	268
	Femur	**Vol. Frac.**	4	17	0	30	10	28	77	42	26	14	38	66	31	47	64	83	120	131	285
		Volume	44	12	46	19	62	61	66	24	13	0	35	59	38	82	108	73	108	132	274
		Thickness	6	10	2	19	21	28	79	32	15	0	31	61	24	48	74	82	117	132	296
		Diameter	43	0	53	27	57	61	69	34	22	10	38	47	44	88	103	76	113	132	279
		pMOI	50	0	58	24	67	67	67	28	16	3	36	48	47	93	113	73	110	135	279
		Imax	45	0	54	25	64	63	76	31	18	5	38	50	47	92	111	81	116	139	295
		Imin	50	0	60	33	69	69	81	36	19	5	39	51	52	99	118	83	121	148	301

Table 2-2. Effect sizes and significance of mass and migratory status (Stat) in explaining length, trabecular morphology, and cortical morphology. Analyses were performed on log-transformed data except for the unitless metrics (volume fraction, structural model index). SMI = Structural Model Index; Stat = migratory status; TMD = tissue mineral density.

			Humerus			Femur		
		Effect	**β ±SE**	**p**		**β ±SE**	**p**	
	Length	Mass	0.211±0.035	<0.001	***	0.240±0.031	<0.001	***
		Stat	-0.014±0.011	0.223		-0.017±0.008	0.049	*
Trabecular	**Volume Fraction**	Mass	0.001±0.001	0.228		0.001±0.001	0.141	
		Stat	-0.009±0.006	0.127		-0.005±0.004	0.269	
	Volume	Mass	0.773±0.283	0.009	**	0.696±0.216	0.002	**
		Stat	-0.092±0.074	0.237		-0.96±0.057	0.110	
	Number	Mass	0.146±0.088	0.102		-0.004±0.080	0.963	
		Stat	0.018±0.022	0.429		0.035±0.020	0.101	
	Thickness	Mass	-0.019±0.135	0.889		-0.067±0.127	0.598	
		Stat	-0.061±0.037	0.123		-0.091±0.039	0.033	*
	SMI	Mass	-0.004±0.014	0.768		-0.007±0.013	0.597	
		Stat	0.066±0.076	0.403		0.076±0.069	0.290	
	Conn. Dens.	Mass	0.374±0.806	0.644		0.908±0.586	0.128	
		Stat	0.189±0.238	0.440		0.399±0.185	0.047	*
Cortical	**Volume Fraction**	Mass	0.000±0.001	0.931		0.000±0.001	0.673	
		Stat	-0.025±0.007	0.002	**	-0.022±0.006	0.001	**
	TMD	Mass	-66.7±142.4	0.614		-56.3±144.0	0.698	
		Stat	-56.1±37.2	0.152		-88.5±36.9	0.030	*
	Volume	Mass	0.756±0.073	<0.001	***	0.638±0.085	<0.001	***
		Stat	-0.012±0.018	0.524		-0.087±0.022	0.001	**
	Thickness	Mass	0.395±0.071	<0.001	***	0.357±0.071	<0.001	***
		Stat	-0.050±0.018	0.013	*	-0.090±0.018	<0.001	***
	Diameter	Mass	0.366±0.035	<0.001	***	0.308±0.044	<0.001	***
		Stat	0.025±0.009	0.016	*	-0.010±0.011	0.382	
	pMOI	Mass	1.413±0.136	<0.001	***	1.199±0.165	<0.001	***
		Stat	0.049±0.035	0.185		-0.103±0.043	0.032	*
	Imax	Mass	1.388±0.139	<0.001	***	1.141±0.168	<0.001	***
		Stat	0.050±0.036	0.187		-0.106±0.044	0.030	*
	Imin	Mass	1.464±0.139	<0.001	***	1.285±0.170	<0.001	***
		Stat	0.050±0.036	0.184		-0.098±0.045	0.047	*

Chapter 3.Microstructure and Mechanical Properties of Bird Bone During Egg-Laying

Introduction

Medullary bone is a woven bone tissue that birds lay down inside their long bones in the weeks prior to laying an egg (Bloom et al., 1941; Taylor and Moore, 1953). It primarily functions as a labile source of calcium during formation of the eggshell (Bloom et al., 1958; Driggers and Comar, 1949; Taylor, 1966). Recent studies have demonstrated that species differ in which bones have or do not have medullary bone (Canoville et al., 2019; Werning, 2018), but it is not clear why species differ. To answer this question, we must know the evolutionary benefits and costs of producing medullary bone. These broadly include: 1) its influence on calcium metabolism during its production and during egg-laying; 2) its influence on whole bone mechanical properties; and 3) its contribution to bone mass and body mass, and consequential influences on energy expenditure and flight mechanics.

Literature to date has focused primarily on how medullary bone varies as a function of calcium homeostasis, especially in poultry (Clunies, Emslie and Leeson, 1992; Dacke et al., 1993; Rennie et al., 1997; Hurwitz and Bar, 2012). While bone plays an important role in calcium homeostasis, it also must remain stiff to protect organs and to resist the large bending and torsional forces applied to it during flight and locomotion (Biewener and Dial, 1995). However, the influence of medullary bone on whole bone mechanical properties is not well known. Medullary bone has been shown to increase whole bone strength (Fleming et al., 1998; Knott and Bailey, 1999; Rath et al., 2000), which would mean that birds with medullary bone are less likely to obtain a fracture under similar conditions. However, others claim that medullary bone may weaken the skeleton by replacing structural bone (Whitehead, 2004), and many authors have stated that medullary bone itself is inherently less stiff and strong than structural bone (Beck and Hansen, 2004; Fleming et al., 2006; Kim et al., 2004; Rath et al., 2000; Riczu et al., 2004). If bones in the wing are less stiff, they will deform more under the same loading forces, which could alter flight mechanics and energetics. Bones that are less stiff and strong will also be more prone to fracture. Most birds continue to forage while medullary bone is present inside their bones, and alterations to whole bone mechanics could influence flight mechanics and the risk of fracture. Therefore, the objective of this study was to understand the structural contribution of medullary bone to whole bone stiffness to determine whether it is a benefit or cost to flight mechanics and energetics.

Production of medullary bone also increases whole bone mass by some 10% (Fleming et al., 1998; Rath et al., 2000). However, the influence of this change on energy requirements has not been explored. Increased bone mass could increase the energy required for flight by increasing inertial power requirements (increased energy to oscillate limbs) and induced power requirements. This increase in energy requirements may require birds to spend more time foraging for food during the critical reproductive period. Therefore, I also consider here how the production of medullary bone could alter bird energy balance and flight mechanics.

To better understand the structural contribution of medullary bone and its influence on flight mechanics and energetics, I created models of long bones with and without medullary bone using

micro-computed tomography (CT) scans. I used male zebra finches (*Taeniopygia guttata*) given an estrogen-eluting implant to create a reliable, repeatable source of medullary bone. I also used females preparing to lay an egg or in the process of laying an egg to confirm that my experiments reflect what occurs naturally. My findings will allow us to identify how medullary bone changes whole bone mechanical properties, and thus will contribute to our understanding of the evolutionary tradeoffs of producing medullary bone. Better knowledge of medullary bone micromechanics may also help us understand calorie requirements and osteoporosis occurrence in laying fowl.

Methods

Subjects

Birds used in this study originated from two captive colonies. One colony housed in a 2.7 m by 2.5 m by 2.1 m indoor flight aviary at the University of California, Berkeley Field Station for the Study of Behavior, Ecology and Reproduction (FSSBER). The remaining 2 females originated from a captive colony housed in a smaller aviary at the University of California, Berkeley (UCB). Birds at FSSBER were exposed to natural changes in day length supplemented by artificial lighting at a light/dark schedule of 12L:12D, while birds at UCB only experienced the artificial lighting schedule. All birds were given ad libitum food and water. During experiments, birds in this study were kept in a separate indoor flight aviary at FSSBER under the same conditions. Experimental procedures for all experiments were approved by the UC Berkeley Institutional Animal Care and Use Committee.

Experimental design

Males. Ten adult male birds were given subcutaneous silastic implants on May 3, 2017. Implants consisted of a 5 mm long silastic tube (i.d. 0.76 mm, o.d. 1.65 mm; 2415542, Dow Corning, Midland, Michigan) packed full of crystalline estradiol (E8875, Sigma-Aldrich, St. Louis, Missouri) (n=6) or left empty as a control (n=4) and sealed using silastic medical adhesive (Type A, Dow Corning, Midland, Michigan). Briefly, the surgical procedure was as follows: 24 hours prior to injection, implants were placed in sterile saline to soak. Each animal was anesthetized using isoflurane and an incision was made between the wing and knee on the animal's right side. The implant was placed under the skin and the incision was closed using Nexaband tissue adhesive. After 2 weeks, animals were euthanized and both humeri and femora were collected for micro-CT scanning. Four individuals from each group were analyzed for this study.

Females. Three experiments were performed as part of a larger study of female bone during egg-laying. In each, an equal number of males and females were housed together in a large flight aviary and checked once daily between 0800-1200 for nest formation and the presence of new eggs. After at least 1 female in an experiment laid an egg, all females were euthanized between 2000-2200 the same day to capture the egg-laying female while she was calcifying a second egg. Reproductive state was identified using the reproductive organs: pre-egg-laying females had ovaries with small yellow or hierarchical ova, while egg-laying females had a partially calcified egg in the uterus. After reproductive state was determined, both humeri and femora were then collected for micro-CT scanning. These experiments occurred from March 1 – 25, 2018 (n=10), June 6 – 22, 2018 (n=4), and August 3 – 26, 2018 (n=10). A subset of 5 birds are analyzed here: 2, 1, and 2 birds from each experiment respectively.

Micro-computed tomography scanning

Left side bones were scanned unless they were broken or missing, in which case right side bones were used. Bones were placed in a 3D-printed specimen tube that held four bones at a time. This tube was placed in a sample holder (o.d. 11.5 mm i.d. 10 mm, U40830, Scanco Medical, Brüttisellen, Switzerland) and filled with saline. Then, micro-CT scans were obtained at an x-ray energy of 70 kVp, integration time of 300 ms, and 6 μm isotropic voxel size (μCT 35, Scanco Medical, Brüttisellen, Switzerland). Two regions were scanned: first, a 0.6 mm long region centered around the center of the midshaft was used in both the humerus and femur to assess the diaphysis. Second, a 0.6 mm long region at one end of each bone was obtained to assess the metaphysis. For the humerus, this region was at the proximal end of the bone, extending distally from the opening of the fossa pneumotricipitalis. For the femur, this region was at the distal end of the bone, extending proximal to the portion of the scan in which both condyles were present.

Model creation

Scans were converted to the DICOM imaging format and imported into MATLAB for model creation. A threshold equivalent to 879 mgHA/cm^3 was applied to all images. Each scan volume was then rotated to ensure that all bones were aligned in the same manner. First, a known linear landmark was found on each bone metaphysis. For the humerus, this feature was the flat plate containing the crista deltopectoralis, crista bicipitalis, and facies bicipitalis, identified using the 'Orientation' property in the regionprops function over 100 slices. For the femur, the plane containing the condyles medialis and condyles lateralis was identified manually on 5 slices. For both the humerus and femur, the scan was then rotated about its transverse axis to orient the landmark feature dorsally. Second, the long axis of the bone was identified in the diaphysis using the 'Centroid' property in the regionprops function, and the scan was rotated to align the long axis of the bone with the transverse axis of the scan. Finally, all bones were cropped so that all analyzed transverse slices were complete. This resulted in a 0.366 mm long region for male bones, and a 0.3120 mm long region for female bones.

To determine the mechanical contribution of medullary bone to whole bone stiffness, medullary bone tissue needed to be digitally removed from models containing it. Medullary bone has the same density as cortical bone (using this scanner and resolution, but see (Fleming et al., 2006)), and therefore a threshold could not be used to distinguish the two bone tissues. Instead, the 3D dataset was opened, closed, and eroded using spherical structuring elements. Since a spherical structuring element does not work well at the edges of a 3D dataset, these operations were performed on the first and last 7 slices using a circular disk structuring element with the same parameters. Medullary bone varied in amount and shape among individual birds, and therefore the radius of the opening, closing, and eroding structuring elements were varied from 0.0120 – 0.0480 mm until the resulting images had similar thicknesses of medullary bone, approximately 0.035 mm. This overestimates the amount of medullary bone, and thus will give a generous estimate of its mechanical properties.

These 2-material images were exported in the DICOM format, loaded into IDL running in Red Hat Linux, and converted to a volume. To ensure that the loading applied results in bending rather than shear, the volume must be at least as long as the bone diameter (Saint-Venant's

principle) (Toupin, 1965). The volume lengths used here were short relative to the bone diameter (for the male humerus: volume length 0.366 mm, average diameter: 1.36 mm), and therefore the bone was mirrored 4 times to increase its length, resulting in a model length of 1.86 mm for males and 1.56 mm for females.

Finite element analyses

***Material properties*.** The whole bone was treated as two materials. Histologically, long bones in small birds are either lamellar or fibrolamellar (Chinsamy and Elzanowski, 2001; de Ricqles et al., 1991; Starck and Chinsamy, 2002) and vascular arrangement is primarily circumferential (de Margerie et al., 2005), potentially as adaptations to torsional loading. Regardless, this suggests that avian bone will deform differently when loaded in a longitudinal, circumferential, or radial direction. However, cortical bone was treated as transversely isotropic (e.g. same material properties in the circumferential and radial directions) due to technical difficulties.

Medullary bone collagen is arranged in a random, isotropic pattern rather than along a longitudinal axis (Candlish and Holt, 1971). Additionally, mineralization in medullary bone does not occur in line with collagen fibrils, but rather in vesicles, resulting in randomly arranged globular structures of mineral (Bonucci and Gherardi, 1975; Yamamoto et al., 2005). Given the random arrangement of collagen and mineral in medullary bone, it was treated as isotropic material.

Boundary conditions. To simulate bending on bone models, the proximal end of the model was fixed and all nodes at the distal end of the bone were displaced by 1% of bone length (0.004 mm for males, 0.003 mm for females). To ensure that plane sections remain plane, the model was constrained from deforming in the cranial-caudal axis, and therefore deformation could only occur along the axis of the bone and in the dorsal-ventral axis.

Morphological data

Custom MATLAB code was used to determine model volume (mm^3) and second moment of area in the axis of bending (I_{xx}, mm^4). Volume and I_{xx} did not differ significantly between empty-implanted males and estrogen-implanted males in which medullary bone was digitally removed, suggesting that models in which medullary bone is digitally removed are good representations of birds in which medullary bone is not present. Given this, the remaining work directly compared each bone against itself with and without medullary bone to directly assess how medullary bone influences whole bone mechanics. To compare the usefulness of medullary bone in contributing to geometric resistance to bending, an efficiency metric was created: $efficiency_{geometric}$, defined as I_{xx}/volume (mm^4/mm^3). Two-tailed paired t-tests implemented in the R-environment (R Core Team, 2018) through R Studio 1.1.456 (RStudio Team, 2015) were used to determine whether volume, I_{xx}, or $efficiency_{geometric}$ changed significantly with the removal of medullary bone.

Stiffness data

To determine the average reaction force experienced by each bone, data were imported into MATLAB. The average shear stress in the yz-direction on all voxels and slices was found and converted into a reaction force (N). This was converted to whole bone stiffness (K, N/mm) by dividing by the displacement applied: 0.0183 mm for males, 0.0156 mm for females. To compare

the ability of bone to resist force when medullary bone is present or absent, an efficiency metric was created: $efficiency_{FEA}$, defined as bone stiffness/volume (K/mm^3). As with the morphological data, two-tailed paired t-tests were used to determine whether stiffness and $efficiency_{FEA}$ changed significantly with the removal of medullary bone. Finally, to determine how much load was held by cortical versus medullary bone, the average load held by each bone type at each slice was determined using custom MATLAB code.

Results

Bone morphology

Averages for all medullary bone parameters are listed in Table 3-1. Medullary bone significantly increased total volume in the male humerus (36%, p=0.002), male femur (41%, p=0.001), and the female humerus (36%, p<0.001) (Figure 3-1a). The presence of medullary bone also yielded significant increases in the relevant second moment of area (I_{xx}) for the male humerus (23%, p=0.010), male femur (29%, 0.004), and female humerus (24%, p=0.001) (Figure 3-1b). Geometric efficiency significantly decreased with the addition of medullary bone in the male humerus (10%, p=0.005), male femur (8%, p=0.003), and female humerus (8%, p=0.004) (Figure 3-1c).

Bone stiffness

Stiffness under a 1% bending displacement increased significantly with the addition of medullary bone in the male humerus (30%, p=0.013), male femur (p=0.028), and female humerus (p<0.001). (Figure 3-1d). $Efficiency_{FEA}$ decreased significantly with the addition of medullary bone in the male femur (12%, p=0.013) and female humerus (5%, p<0.001). It also decreased in the male humerus, but the change was not significant (5%, p=0.053) (Figure 3-1e).

Load sharing

Medullary bone occupied an average of 26% of the male humerus, 29% of the male femur, and 26% in the female humerus. It held a slightly smaller portion of the load: 25% in the male humerus, 23% in the male femur, and 24% in the female humerus (Figure 3-2). Its presence also resulted in a decrease in the load held in the cortex by 6% in the male humerus, 7% in the male femur, and 2% in the female humerus.

Discussion

This study addressed the question of how medullary bone influences whole bone microarchitecture, and the resulting influences on mechanical properties and flight mechanics. My results showed that a 36 – 41% increase in bone volume leads to only a 24 – 30% increase in whole bone stiffness. This resulted in a decrease in $efficiency_{geometric}$ by 8 – 10% and $efficiency_{FEA}$ by 5 – 12%. Therefore, addition of bone volume as medullary bone does not lead to a concomitant increase in resistance to bending, and medullary bone is not an optimum use of material in terms of increasing bending stiffness. In other words, medullary bone does not significantly change whole bone stiffness. The findings of this study align with previous work by (Fleming et al., 1998a) who showed that an increase in bone mass of 13% led to only a 5.8% increase in breaking force in bending for birds with a medullary bone score of 2, and by other

studies that show that medullary bone is not as strong as structural bone (Fleming et al., 1996; Fleming et al., 1998a; Knott and Bailey, 1999).

The fact that medullary bone does not change whole bone stiffness means that it should minimally alter flight mechanics and energetics. That is, wing bones with medullary bone will deform similarly during flight to those without medullary bone, resulting in similar muscle requirements and therefore similar amounts of energy required to fly.

Influence of medullary bone on whole bone loading

Additionally, although medullary bone occupies some 26 – 29% of bone volume in our study, it only reduces the loading experienced in the cortical bone by 2 – 7%. Therefore, this placement of large quantities of bone ensures that cortical loading is maintained and minimizes the chance of cortical resorption as a result of reduced loading. If mechanical loading remains the same, bone mass and thus whole bone mechanical properties will be maintained (Lanyon and Rubin, 1984). In contrast, reduced loading can result in bone resorption and diminished mechanical properties (Biewener and Bertram, 1994; Ellman et al., 2013; Shipov et al., 2010). Therefore, maintenance of mechanical loading during egg-laying may ensure that whole bone mechanical properties will be the same after egg-laying. Further, some studies have shown that birds lose structural bone in the process of forming medullary bone (Fleming et al., 1998b; Taylor and Moore, 1954; Turner et al., 1993; Wilson and Thorp, 1998). If this loss in bone mass is similar to the 2 – 7% decrease in cortical loading shown here, cortical loading may be fully maintained during egg-laying.

Given that medullary bone increases bone volume by 36 – 41% but minimally alters bending stiffness and cortical loading, it represents an ideal compromise between the need to store calcium for use during egg-laying while maintaining bone loading and bone mechanical integrity. This work therefore confirms the primary role of medullary bone to store calcium during egg-laying, as stated by many previous authors (Bloom et al., 1958; Comar and Driggers, 1949; Taylor, 1966). Further, my work demonstrates that medullary bone microstructure minimizes the potentially negative side effects of drastically increasing bone mass. This means that the bone morphology prior to egg-laying should be fully maintained during egg-laying, and therefore the bird should be able to quickly regain its original bone stiffness and bone strength after egg-laying. This is especially important because after laying an egg, birds must continue to forage and survive to keep the egg warm.

Structural and material properties of medullary bone

The reduction in efficiency$_{FEA}$ of 5 – 12% is similar to the 14% decrease we can calculate for birds with a medullary bone score of 2 in the study by Fleming and coauthors (1998). Since I modeled medullary bone using similar material properties to those for structural bone, this reduced efficiency can be explained by morphological factors: first, medullary bone is placed on the interior surface of the bone, very close to the neutral axis of bending, and thus is not in an ideal location for resisting bending forces. Second, medullary bone is laid down in thin struts or spicules, rather than as complete sheets of bone. Although the spicules hold force, they are not able to transfer load along the bone as easily as continuous sheets of bone.

Some workers have suggested that medullary bone is inherently weaker because of its differences in material makeup (Knott and Bailey, 1999; Whitehead, 2004). These differences include that medullary bone mineral crystals are arranged in globules rather than along collagen fibrils, that it has reduced collagen content but increased proteoglycan content, that it lacks lamellar arrangement, and that it differs in cross-linking relative to structural bone (Ascenzi et al., 1963; Candlish, 1971; Candlish and Holt, 1971; Knott and Bailey, 1999; Yamamoto et al., 2005). However, given that the reduced efficiency found here is similar to that observed in mechanical tests of medullary bone, and given that the material properties of medullary and structural bone were similar in this study, my work shows that it is microstructure, not material makeup, that gives medullary bone its poor mechanical advantage. A potential explanation lies in the theory that bone stiffness (e.g. pre-yield mechanical properties) is primarily determined by the mineral content of bone, while ductility (e.g. post-yield mechanical properties) is primarily determined by organic components (Burstein et al., 1975). Since medullary bone has similar mineral content to structural bone, it provides similar resistance to mechanical loading, despite differences in the content and arrangement of its organic material.

Influence of medullary bone on flight mechanics and energetics

I also wondered whether the 36 – 41% increase in bone mass that I observed might significantly increase induced and/or inertial power requirements. Skeletal mass in small passerine birds is typically about 5% of total body mass (Prange et al., 1979). Since induced power scales approximately with bird mass$^{3/2}$, this will result in an increase in power by only 3%. Inertial power depends on wing moment of inertia, which is proportional mass $\times$ distance^2. In birds, wing moment of inertia is bell-shaped, as heavy bone and mass are located proximally in order to minimize the moment of inertia (Berg and Rayner, 1995). Further, muscle contributes far more to total mass than bone, at 30% in most birds (Lindström et al., 2000). Given its proximal distribution and proportionally small contribution to wing mass, a 40% increase in bone mass will only increase inertial power requirements by around 4%. Although small, these increases in power requirements will increase the energy a bird needs to consume a time when nutrient requirements are high in order to create eggs. This may partially explain why some species increase nutrient storage prior to laying an egg (Perrins, 1980).

Conclusion

Medullary bone formation increased bone mass by 36 – 41% but increased whole bone stiffness in bending by only 24 – 30%. Its inefficiency is due to its placement and its spicule-like microstructure, rather than its material properties. It also had minimal influences on load held in the cortex. It thus represents an ideal compromise between the need to store calcium for use during egg-laying while maintaining bone loading and bone mechanical integrity.

Figures

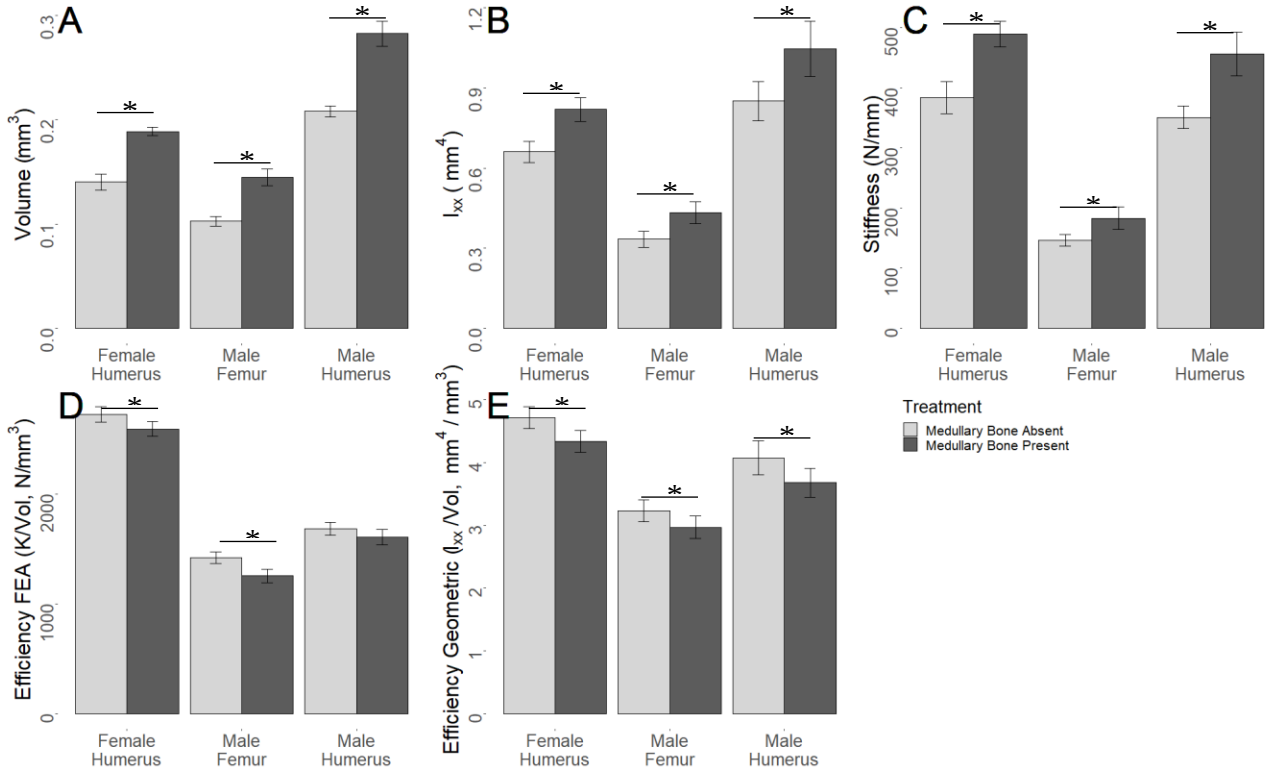

Figure 3-1. Geometric and loading properties in the female humerus during egg laying and in the estrogen-implanted male femur and humerus when medullary bone is present or absent. Volume (A), second moment of area (B), stiffness (C), efficiency as determined using bone stiffness relative to volume (D), and efficiency as determined using second moment of area relative to volume (E). For each bone type, results are shown in which medullary bone was virtually removed or kept in the model. Error bars indicate standard error. An asterisk (*) indicates a significant difference ($p<0.05$) between the bars.

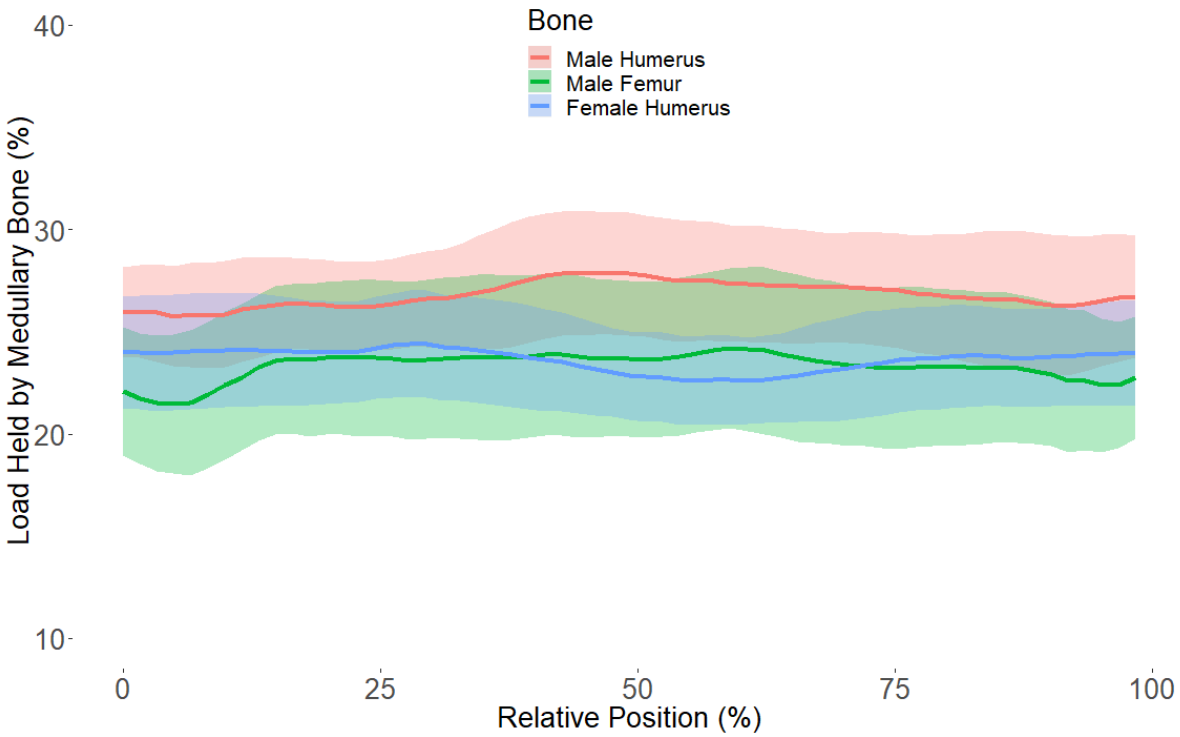

Figure 3-2. Proportion of load held by medullary as a function of position (proximal to distal) in the model. Results are shown for the estrogen-implanted male humerus and femur as well as the female humerus during egg-laying. The shaded area around each line indicates standard error.

Tables

Table 3-1. Morphological parameters and finite element analysis results for estrogen-implanted male humeri and femurs and for female humeri during egg-laying with and without medullary bone.

	MEDULLARY BONE ABSENT			MEDULLARY BONE PRESENT		
	Volume [mm^3]	**I_{xx} [mm^4]**	**Efficiency [N mm^{-3}]**	**Volume [mm^3]**	**I_{xx} [mm^3]**	**Efficiency [N mm^{-3}]**
MALE HUMERUS						
53	0.214	0.854±0.006	-31.68	0.289	1.031±0.011	-22.20
54	0.203	0.877±0.003	-32.41	0.285	1.127±0.005	-28.39
55	0.196	0.657±0.006	-27.57	0.249	0.767±0.010	-19.83
56	0.219	1.014±0.016	-31.54	0.307	1.260±0.011	-31.22
Average	**0.209±0.008**	**0.897±0.147**	**30.80±1.89**	**0.282±0.021**	**1.046±0.225**	**29.40±2.17**
MALE FEMUR						
53	0.106	0.277±0.004	-24.83	0.146	0.349±0.006	-21.54
54	0.114	0.375±0.007	-27.08	0.165	0.487±0.007	-25.66
55	0.092	0.253±0.007	-24.06	0.126	0.315±0.008	-20.65
58	0.099	0.330±0.005	-28.09	0.141	0.439±0.010	-24.01
Average	**0.103±0.008**	**0.333±0.050**	**26.01±1.64**	**0.145±0.014**	**0.432±0.071**	**22.96±1.98**
FEMALE HUMERUS						
109	0.148	0.734±0.007	-45.60	0.193	0.898±0.009	-35.70
110	0.140	0.670±0.009	-41.62	0.188	0.830±0.007	-32.77
112	0.139	0.719±0.007	-44.14	0.193	0.921±0.012	-35.36
115	0.161	0.673±0.005	-41.91	0.195	0.774±0.006	-34.81
116	0.114	0.509±0.016	-39.31	0.173	0.675±0.017	-32.94
Average	**0.140±0.015**	**0.661±0.080**	**42.52±2.17**	**0.189±0.008**	**0.819±0.089**	**40.42±2.09**

References

Aleixandre, P., Milá, B., Navarro-Sigüenza, A. G., Friis, G. and Rodríguez-Estrella, R. (2016). Rapid postglacial diversification and long-term stasis within the songbird genus Junco : phylogeographic and phylogenomic evidence . *Mol. Ecol.* **25**, 6175–6195.

Altshuler, D. L. and Dudley, R. (2002). The ecological and evolutionary interface of hummingbird flight physiology. *J. Exp. Biol.* **205**, 2325–36.

Altshuler, D. L., Princevac, M., Pan, H. and Lozano, J. (2009). Wake patterns of the wings and tail of hovering hummingbirds. *Exp. Fluids* **46**, 835–846.

Anderson, B., Cole, W. W. and Barrett, S. C. H. (2005). Specialized bird perch aids cross-pollination. *Nature* **435**, 41–42.

Ascenzi, A., Francois, C. and Bocciarelli, D. S. (1963). On the bone induced by estrogens in birds. *J. Ultrastruct. Res.* **8**, 491–505.

Battley, P. F. and Piersmazs, T. (1997). Body composition of Lesser Knots (Calidris canutus rogersi) preparing to take off on migration from northern New Zealand. *J. Ornithol. Soc. New Zeal.* **44**, 137–150.

Beck, M. M. and Hansen, K. K. (2004). Role of estrogen in avian osteoporosis. *Poult. Sci.* **83**, 200–206.

Berg, C. and Rayner, J. (1995). The moment of inertia of bird wings and the inertial power requirement for flapping flight. *J. Exp. Biol.* **198**, 1655–64.

Biebach, H. (1998). Phenotypic Organ Flexibility in Garden Warblers Sylvia borin during Long-Distance Migration. *J. Avian Biol.* **29**, 529–535.

Biewener, A. A. and Bertram, J. E. (1994). Structural response of growing bone to exercise and disuse. *J. Appl. Physiol.* **76**, 946–955.

Biewener, A. A. and Dial, K. P. (1995). In vivo strain in the humerus of pigeons (Columba livia) during flight. *J. Morphol.* **225**, 61–75.

Blob, R. W., Espinoza, N. R., Butcher, M. T., Lee, A. H., D'Amico, A. R., Baig, F. and Sheffield, K. M. (2014). Diversity of Limb-Bone Safety Factors for Locomotion in Terrestrial Vertebrates: Evolution and Mixed Chains. *Integr. Comp. Biol.* **54**, 1–14.

Bloom, W., Bloom, M. A. and McLean, F. C. (1941). Calcification and ossification: medullary bone changes in the reproductive cycle of female pigeons. *Anat. Rec.* **81**, 443–475.

Bloom, M. A., Domm, L. V, Nalbandov, A. V and Bloom, W. (1958). Medullary bone of laying chickens. *Am. J. Anat.* **102**, 411–453.

Bollback, J. P. (2006). SIMMAP: Stochastic character mapping of discrete traits on phylogenies. *BMC Bioinformatics* **7**, 1–7.

Bonucci, E. and Gherardi, G. (1975). Histochemical and electron microscope investigations on medullary bone. *Cell Tissue Res.* **163**, 81–97.

Bouxsein, M. L., Boyd, S. K., Christiansen, B. a, Guldberg, R. E., Jepsen, K. J. and Müller, R. (2010). Guidelines for assessment of bone microstructure in rodents using micro-computed tomography. *J. Bone Miner. Res.* **25**, 1468–86.

Bowie, R. C. K., Fjeldså, J., Hackett, S. J. and Crowe, T. M. (2004). Systematics and biogeography of Double-Collared Sunbirds from the Eastern Arc Mountains, Tanzania. *Auk* **121**, 660–681.

Bowie, R. C. K., Fjeldså, J., Kiure, J. and Kristensen, J. B. (2016). A new member of the greater double-collared sunbird complex (Passeriformes: Nectariniidae) from the Eastern Arc Mountains of Africa. *Zootaxa* **4175**, 23–42.

Brown, R. H. J. (1963). The flight of birds. *Biol. Rev.* **38**, 460–489.

Burnham, K. P. and Anderson, D. R. (2002). *Model Selection and Multimodel Inference*. Second. New York: Springer.

Burr, D. B. (1997). Muscle strength, bone mass, and age-related bone loss. *J. Bone Miner. Res.* **12**, 1547–1551.

Burstein, A. H., Zika, J. M., Heiple, K. G. and Klein, L. (1975). Contribution of collagen and mineral to the elastic-plastic properties of bone. *1The J. Bone Jt. Surg.* **57**,.

Candlish, J. K. (1971). The collagen fibrils in fowl medullary bone. *Br. Poult. Sci.* **12**, 111–117.

Candlish, J. K. and Holt, F. J. (1971). The proteoglycans of fowl cortical and medullary bone. *Comp. Biochem. Physiol. -- Part B Biochem.* **40**, 283–290.

Canoville, A., Schweitzer, M. H. and Zanno, L. E. (2019). Systemic distribution of medullary bone in the avian skeleton: ground truthing criteria for the identification of reproductive tissues in extinct Avemetatarsalia. *BMC Evol. Biol.* **19**, 1–20.

Chamay, A. (1970). Mechanical and morphological aspects of experimental overload and fatigue in bone. *J. Biomech.* **3**,.

Chandler, C. R. and Mulvihill, R. S. (1990). Wing-shape variation and differential timing of migration in dark-eyed juncos. *Condor* **92**, 54–61.

Chang, Y. H., Ting, S. C., Liu, C. C., Yang, J. T. and Soong, C. Y. (2011). An unconventional mechanism of lift production during the downstroke in a hovering bird (Zosterops japonicus). *Exp. Fluids* **51**, 1231–1243.

Chang, Y.-H., Ting, S.-C., Su, J.-Y., Soong, C.-Y. and Yang, J.-T. (2013). Ventral-clap modes of hovering passerines. *Phys. Rev. E* **87**, 1–11.

Cheke, R. A. and Mann, C. F. (2001). *Sunbirds: A Guide to the Sunbirds, Flowerpeckers, Spiderhunters and Sugarbirds of the World*. New Haven, CT: Yale University Press.

Cheke, R. A. and Mann, C. F. (2008a). Family Dicaeidae (Flowerpeckers). In *Handbook of the Birds of the World* (ed. del Hoyo, J.), Elliott, A.), and Christie, D. A.), pp. 350–389. Barcelona: Lynx Edicions.

Cheke, R. A. and Mann, C. (2008b). Family Nectariniidae (Sunbirds). In *Handbook of the Birds of the World* (ed. del Hoyo, J.), Elliott, A.), and Christie, D. A.), pp. 196–320. Barcelona: Lynx Edicions Family.

Chinsamy, A. and Elzanowski, A. (2001). Evolution of growth pattern in birds. *Nature* **412**, 402–403.

Clark, C. J. (2010). The evolution of tail shape in hummingbirds. *Auk* **127**, 44–56.

Clark, C. J. and Dudley, R. (2009). Flight costs of long, sexually selected tails in hummingbirds. *Proc. Biol. Sci.* **276**, 2109–15.

Collins, B. G. and Paton, D. C. (1989). Consequences of differences in body mass, wing length and leg morphology for nectar-feeding birds. *Aust. J. Ecol.* **14**, 269–289.

Comar, C. L. and Driggers, J. C. (1949). Secretion of radioactive calcium in the hen's egg. *Science (80-.).* **109**, 282.

Coss, D., Yang, L., Kuo, C. B., Xu, X., Luben, R. A. and Walker, A. M. (2017). Effects of prolactin on osteoblast alkaline phosphatase and bone formation in the developing rat. *Am. J. Physiol. Metab.* **279**, E1216–E1225.

Dacke, C. G., Sugiyama, T. and Gay, C. V. (2015). The role of hormones in the regulation of bone turnover and eggshell calcification. In *Sturkie's Avian Physiology* (ed. Scanes, C. G.), pp. 549–575. San Francisco: Elsevier.

Dawson, W. R., Marsh, R. L. and Yacoe, M. E. (1983). Metabolic adjustments of small passerine birds for migration and cold. *Am. J. Physiol.* **245**, R755–R767.

de Margerie, E., Sanchez, S., Cubo, J. and Castanet, J. (2005). Torsional resistance as a principal component of the structural design of long bones: comparative multivariate evidence in birds. *Anat. Rec. A. Discov. Mol. Cell. Evol. Biol.* **282A**, 49–66.

de Ricqles, A., Meunier, F. J., Castanet, J. and Francillon-Viellot, H. (1991). Comparative Microstructure of Bone. In *Bone* (ed. Hall, B. K.), pp. 1–78. Ann Arbor: CRC Press.

Driggers, J. C. and Comar, C. L. (1949). The secretion of radioactive calcium (Ca45) in the hen's egg. *Poult. Sci.* **28**, 420–424.

Dunning, J. B. J. (2008). *CRC Handbook of Avian Body Masses Second Edition*. Second. New York: Taylor & Francis Group.

Ellman, R., Spatz, J., Cloutier, A., Palme, R., Christiansen, B. A. and Bouxsein, M. L. (2013). Partial reductions in mechanical loading yield proportional changes in bone density, bone architecture, and muscle mass. *J. Bone Miner. Res.* **28**, 875–885.

Fleming, R. H., Mccormack, H. A., Mcteir, L. and Whitehead, C. C. (1996). Influence of medullary bone on humeral breaking strength. *Br. Poult. Sci.* **37**, S30–S32.

Fleming, R. H., McCormack, H. A., McTeir, L. and Whitehead, C. C. (1998a). Medullary bone and humeral breaking strength in laying hens. *Res. Vet. Sci.* **64**, 63–7.

Fleming, R. H., McCormack, H. A. and Whitehead, C. C. (1998b). Bone structure and strength at different ages in laying hens. *Br. Poult. Sci.* **39**, 434–440.

Fleming, R. H., McCormack, H. A., McTeir, L. and Whitehead, C. C. (2006). The relative density of bone types in laying hens. *Proc. XIIth Eur. Poult. Conf. Verona, Italy, 10th—14th Sept.*

Freckleton, R. P., Harvey, P. H. and Pagel, M. (2002). Phylogenetic Analysis and Comparative Data: A Test and Review of Evidence. *Am. Nat.* **160**, 712–726.

Geerts, S. and Pauw, A. (2009). African sunbirds hover to pollinate an invasive hummingbird-pollinated plant. *Oikos* **118**, 573–579.

Greenewalt, C. H. (1962). *Dimensional relationships for flying animals*. Smithsonian Miscellaneous Collections.

Greenewalt, C. (1975). The flight of birds: the significant dimensions, their departure from the requirements for dimensional similarity, and the effect on flight aerodynamics of that departure. *Trans. Am. Philos. Soc.* **65**, 1–67.

Guo, X. E. (2001). Mechanical Properties of Cortical Bone and Cancellous Bone Tissue. In *Bone mechanics handbook*, pp. 1–23.

Hainsworth, F. R. and Wolf, L. L. (1972). Power for hovering flight in relation to body size in hummingbirds. *Am. Nat.* **106**, 589–596.

Hamilton, T. H. (1961). The adaptive significances of intraspecific trends of variation in wing engths and body size among bird species. *Evolution (N. Y).* **15**, 180–195.

Hansen, T. F. (2006). Stabilizing Selection and the Comparative Analysis of Adaptation. *Evolution (N. Y).* **51**, 1341.

Hester, P. Y., Schreiweis, M. A., Orban, J. I., Mazzuco, H., Kopka, M. N., Ledur, M. C. and Moody, D. E. (2004). Assessing bone mineral density in vivo: Dual energy X-ray absorptiometry. *Poult. Sci.* **83**, 215–221.

Higgins, P. J., Christidis, L. and Ford, H. A. (2008). Family Meliphagidae (Honeyeaters). In *Handbook of the* (ed. del Hoyo, J.), Elliott, A.), and Christie, D. A.), pp. 498–691. Barcelona: Lynx Edicions.

Hobbhahn, N. and Johnson, S. D. (2015). Sunbird pollination of the dioecious root parasite Cytinus sanguineus (Cytinaceae). *South African J. Bot.* **99**, 138–143.

Holberton, R. L., Boswell, T. and Hunter, M. J. (2008). Circulating prolactin and corticosterone concentrations during the development of migratory condition in the Dark-eyed Junco, Junco hyemalis. *Gen. Comp. Endocrinol.* **155**, 641–649.

Ingersoll, R., Haizmann, L. and Lentink, D. (2018). Biomechanics of hover performance in Neotropical hummingbirds versus bats.

Janeček, Š., Patáčová, E., Bartoš, M., Padyšáková, E., Spitzer, L. and Tropek, R. (2011). Hovering sunbirds in the Old World: occasional behaviour or evolutionary trend? *Oikos*

120, 178–183.

Johnson, S. D. (1996). Bird pollination in South African species of Satyrium (Orchidaceae). *Plant Syst. Evol.* **203**, 91–98.

Johnson, S. D. and Brown, M. (2004). Transfer of pollinaria on birds' feet: A new pollination system in orchids. *Plant Syst. Evol.* **244**, 181–188.

Kim, W. K., Ford, B. C., Mitchell, A. D., Elkin, R. G. and Leach, R. M. (2004). Comparative assessment of bone among wild-type, restricted ovulator and out-of-production hens. *Br. Poult. Sci.* **45**, 463–470.

Knott, L. and Bailey, a J. (1999). Collagen biochemistry of avian bone: comparison of bone type and skeletal site. *Br. Poult. Sci.* **40**, 371–379.

Kodama, Y., Umemura, Y., Nagasawa, S., Beamer, W. G., Donahue, L. R., Rosen, C. R., Baylink, D. J. and Farley, J. R. (2000). Exercise and mechanical loading increase periosteal bone formation and whole bone strength in C57BL/6J mice but not in C3H/Hej mice. *Calcif. Tissue Int.* **66**, 298–306.

Krishnamra, N. and Seemoung, J. (2011). Effects of acute and long-term administration of prolactin on bone 45 Ca uptake, calcium deposit, and calcium resorption in weaned, young, and mature rats . *Can. J. Physiol. Pharmacol.* **74**, 1157–1165.

Lanyon, L. E. and Rubin, C. T. (1984). Static vs dynamic loads as an influence on bone remodelling. *J. Biomech.* **17**, 897–905.

Launey, M. E., Buehler, M. J. and Ritchie, R. O. (2010). *On the Mechanistic Origins of Toughness in Bone*.

Lindström, Å., Kvist, A., Piersma, T., Dekinga, A. and Dietz, M. W. (2000). Avian pectoral muscle size rapidly tracks body mass changes during flight, fasting and fuelling. *J. Exp. Biol.* **203**, 913–919.

Lotinun, S., Limlomwongse, L., Sirikulchayanonta, V. and Krishnamra, N. (2003). Bone calcium turnover, formation, and resorption in bromocriptine- and prolactin-treated lactating rats. *Endocrine* **20**, 163–170.

Marsh, R. L. (1984). Adaptations of the gray catbird Dumetella carolinensis to long-distance migration: flight muscle hypertrophy associated with elevated body mass. *Physiol. Zool.* **57**, 105–117.

Martins, E. P. and Hansen, T. F. (1997). Phylogenies and the comparative method: a general approach to incorporating phylogenetic information into the analysis of interspecific data. *Am. Nat.* **149**, 646–667.

Meaney, A. M., Smith, S., Howes, O. D., O'Brien, M., Murray, R. M. and O'Keane, V. (2004). Effects of long-term prolactin-raising antipsychotic medication an bone mineral density in patients with schizophrenia. *Br. J. Psychiatry* **184**, 503–508.

Meier, A. H., Farner, D. S. and King, J. R. (1965). A possible endocrine basis for migratory

behaviour in the White-crowned Sparrow, Zonotrichia leucophrys gambelii. *Anim. Behav.* **13**, 453–465.

Morey-Holton, E. R. and Globus, R. K. (1998). Hindlimb unloading of growing rats: A model for predicting skeletal changes during space flight. *Bone* **22**, 83–88.

Muijres, F. T., Bowlin, M. S., Johansson, L. C. and Hedenstrom, A. (2012). Vortex wake, downwash distribution, aerodynamic performance and wingbeat kinematics in slow-flying pied flycatchers. *J. R. Soc. Interface* **9**, 292–303.

Mulvihill, R. S. and Chandler, C. R. (1991). A comparison of wing shape between migratory and sedentary Dark-Eyed Juncos (Junco hyemalis). *Condor* **93**, 172–175.

Nazarian, A., Snyder, B. D., Zurakowski, D. and Müller, R. (2008). Quantitative micro-computed tomography: A non-invasive method to assess equivalent bone mineral density. *Bone* **43**, 302–311.

Nolan, Jr., V. and Ketterson, E. D. (1983). An Analysis of Body Mass, Wing Length, and Visible Fat Deposits of Dark-Eyed Juncos Wintering at Different Latitudes. *Wilson Bull.* **95**, 603–620.

Nolan, Jr., V., Ketterson, E. D., Cristol, D. A., Rogers, C. M., Clotfelter, E. D., Titus, R. C., Schoech, S. J. and Snajdr, E. (2002). Dark-eyed Junco (Junco hyemalis). *Birds North Am.*

Nolan, V. and Ketterson, E. D. (1990). Timing of autumn migration and its relation to winter distribution in dark-eyed juncos. *Ecology* **71**, 1267–1278.

Norberg, U. M. (1990). *Vertebrate Flight: Mechanics, Physiology, Morphology, Ecology and Evolution*. New York: Springer-Verlag.

Orava, S., Puranen, J. and Ala-Ketola, L. (1978). Stress fractures caused by physical exercise. *Acta Orthop.* **49**, 19–27.

Pagel, M. (1999). Inferring the historical patterns of biological evolution. *Nature* **401**, 877–884.

Paradis, E., Claude, J. and Strimmer, K. (2004). APE: Analyses of phylogenetics and evolution in R language. *Bioinformatics* **20**, 289–290.

Perrins, C. M. (1980). Eggs, egg formation and the timing of breeding. *Ibis (Lond. 1859).* **138**, 2–15.

Piersma, T. and Gill, R. E. (1998). Guts don't fly: small digestive organs in obese bar-tailed godwits. *Auk* **115**, 196–203.

Pinheiro, J., Bates, D., S, D., D, S. and R Core Team (2019). nlme: Linear and nonlinear mixed effects models.

Posada, D. (1998). Selecting models of evolution. In *The Phylogenetic Handbook: A Practical Approach to Phylogenetic Analysis and Hypothesis Testing* (ed. Lemey, P.), Salemi, M.), and Vandamme, A.-M.), pp. 345–361. New York: Cambridge University Press.

Posada, D. and Buckley, T. R. (2004). Model selection and model averaging in phylogenetics:

Advantages of Akaike Information Criterion and Bayesian approaches over likelihood ratio tests. *Syst. Biol.* **53**, 793–808.

Prange, H. D., Anderson, J. F. and Rahn, H. (1979). Scaling of skeletal mass to body mass in birds and mammals. *Am. Nat.* **113**, 103–122.

R Core Team (2018). A language and environment for statistical computing. *R Found. Stat. Comput.*

Rath, N. C., Huff, G. R., Huff, W. E. and Balog, J. M. (2000). Factors regulating bone maturity and strength in poultry. *Poult. Sci.* **79**, 1024–1032.

Reilly, G. C. and Currey, J. D. (2000). The effects of damage and microcracking on the impact strength of bone. *J. Biomech.* **33**, 337–343.

Revell, L. J. (2009). Size-correction and principal components for interspecific comparative studies. *Evolution (N. Y).* **63**, 3258–3268.

Revell, L. J. (2012). phytools: An R package for phylogenetic comparative biology (and other things). *Methods Ecol. Evol.* **3**, 217–223.

Revell, L. J. (2013). Two new graphical methods for mapping trait evolution on phylogenies. *Methods Ecol. Evol.* **4**, 754–759.

Riczu, C. M., Saunders-Blades, J. L., Yngvesson, Ић K, Robinson, F. E. and Korver, D. R. (2004). End-of-cycle bone quality in white-and brown-egg laying hens. *Poult. Sci.* **83**, 375–383.

RStudio Team (2015). RStudio: Integrated Development for R.

Rubin, C. T. and Lanyon, L. E. (1984). Regulation of bone formation by applied dynamic loads. *J. Bone Jt. Surg.* **66A**, 397–402.

Rubin, C. T. and Lanyon, L. E. (1985). Regulation of bone mass by mechanical strain magnitude. *Calcif. Tissue Int.* **37**, 411–417.

Schaffler, M. B., Radin, E. L. and Burr, D. B. (1989). Mechanical and morphological effects of strain rate on fatigue of compact bone. *Bone* **10**, 207–214.

Schaffler, M. B., Choi, K. and Milgrom, C. (1995). Aging and matrix microdamage accumulation in human compact bone. *Bone* **17**, 521–525.

Shipov, A., Sharir, A., Zelzer, E., Milgram, J., Monsonego-Ornan, E. and Shahar, R. (2010). The influence of severe prolonged exercise restriction on the mechanical and structural properties of bone in an avian model. *Vet. J.* **183**, 153–160.

Skandalis, D. A., Segre, P. S., Bahlman, J. W., Groom, D. J. E., Welch, K. C., Witt, C. C., McGuire, J. A., Dudley, R., Lentink, D. and Altshuler, D. L. (2017). The biomechanical origin of extreme wing allometry in hummingbirds. *Nat. Commun.* **8**, 1–8.

Skead, C. J. (1967). *The Sunbirds of Southern Africa. South African Bird Book Fund: Amsterdam.*

Starck, J. M. and Chinsamy, A. (2002). Bone microstructure and developmental plasticity in birds and other dinosaurs. *J. Morphol.* **254**, 232–246.

Stiles, F., Altshuler, D. L., Dudley, R. and Johnson, K. (2005). Wing morphology and flight behavior of some North American hummingbird species. *Auk* **122**, 872–886.

Su, J.-Y., Ting, S.-C., Chang, Y.-H. and Yang, J.-T. (2011). Aerodynamic trick for visual stabilization during downstroke in a hovering bird. *Phys. Rev. E* **84**, 012901.

Su, J.-Y., Ting, S.-C., Chang, Y.-H. and Yang, J.-T. (2012). A passerine spreads its tail to facilitate a rapid recovery of its body posture during hovering. *J. R. Soc. Interface* **9**, 1674–84.

Suarez, R. K., Lighton, J. R., Brown, G. S. and Mathieu-Costello, O. (1991). Mitochondrial respiration in hummingbird flight muscles. *Proc. Natl. Acad. Sci. U. S. A.* **88**, 4870–3.

Symonds, M. R. E. and Blomberg, S. P. (2014). Chapter 5: A Primer on Phylogenetic Generalised Least Squares. In *Modern Phylogenetic Comparative Methods and their Application in Evolutionary Biology*, pp. 105–130.

Taylor, T. G. (1966). The endocrine control of calcium metabolism in the fowl. In *Physiology of the domestic fowl* (ed. Horton-Smith, C.) and Amoroso, E. C.), pp. 199–202. Edinburgh: Oliver & Boyd.

Taylor, T. G. and Moore, J. H. (1953). Avian medullary bone. *Nature* **172**, 504–505.

Taylor, T. G. and Moore, J. H. (1954). Skeletal depletion in hens laying on a low-calcium diet. *Br. J. Nutr.* **8**, 112–24.

Thomas, A. L. R. and Balmford, A. (1995). How natural selection shapes birds' tails. *Am. Nat.* **146**, 848–868.

Tingley, M. W., Monahan, W. B., Beissinger, S. R. and Moritz, C. (2009). Birds track their Grinnellian niche through a century of climate change. *Proc. Natl. Acad. Sci.* **106**, 19637–19643.

Tingley, M. W., Koo, M. S., Moritz, C., Rush, A. C. and Beissinger, S. R. (2012). The push and pull of climate change causes heterogeneous shifts in avian elevational ranges. *Glob. Chang. Biol.* **18**, 3279–3290.

Toupin, R. A. (1965). Saint-Venant's Principle. *Arch. Ration. Mech. Anal.* **18**, 83–96.

Traylor, M. A. (1950). Altitudinal variation in Bolivian birds. *Condor* **52**, 123–126.

Tromp, A. M., Bravenboer, N., Tanck, E., Oostlander, A., Holzmann, P. J., Kostense, P. J., Roos, J. C., Burger, E. H., Huiskes, R. and Lips, P. (2006). Additional weight bearing during exercise and estrogen in the rat: The effect on bone mass, turnover, and structure. *Calcif. Tissue Int.* **79**, 404–415.

Turner, R. C. and Midgley, J. J. (2016). Sunbird-pollination in the geoflorous species Hyobanche sanguinea (Orobanchaceae) and Lachenalia luteola (Hyacinthaceae). *South African J. Bot.* **102**, 186–189.

Turner, R. T., Bell, N. B. and Gay, C. V. (1993). Evidence that estrogen binding sites are present in bone cells and mediate medullary bone formation in Japanese quail. *Poult. Sci.* **72**, 728–740.

Van der Niet, T., Cozien, R. J. and Johnson, S. D. (2015). Experimental evidence for specialized bird pollination in the endangered South African orchid Satyrium rhodanthum and analysis of associated floral traits. *Bot. J. Linn. Soc.* **177**, 141–150.

Werning, S. (2018). Medullary bone is phylogenetically widespread and its skeletal distribution varies by taxon. *J. Ornithol.* **159**, 527–543.

Wester, P. (2013a). Feeding on the wing: hovering in nectar-drinking Old World birds–more common than expected. *Emu* **114**, 171–183.

Wester, P. (2013b). Sunbirds hover at flowers of Salvia and Lycium. *Ostrich J. African Ornithol.* **84**, 27–32.

Whitehead, C. C. (2004). Overview of bone biology in the egg-laying hen. *Poult. Sci.* **83**, 193–199.

Wikelski, M., Tarlow, E. M., Raim, A., Diehl, R. H., Larkin, R. P. and Visser, G. H. (2003). Costs of migration in free-flying songbirds. *Nature* **423**, 2003.

Wilson, S. and Thorp, B. H. (1998). Estrogen and cancellous bone loss in the fowl. *Calcif. Tissue Int.* **62**, 506–511.

Wingfield, J. C., Schwabl, H. and Mattocks Jr., P. W. (1990). Endocrine mechanisms of migration. In *Bird migration: Physiology and ecology.* (ed. Gwinner, E.), pp. 232–256. New York.

Wolfson, A. (1945). The role of the pituitary, fat deposition, and body weight in bird migration. *Condor* **47**, 95–127.

Yamamoto, T., Nagaoka, N., Hirata, A., Nakamura, H., Inoue, M., Kawai, M. and Ikegame, M. (2005). Ultrastructural and immunohistochemical studies of medullary bone calcification, with special reference to sulphated glycosaminoglycans. *J. Electron Microsc. (Tokyo).* **54**, 29–34.

Zusi, R. L. (2013). Introduction to the skeleton of hummingbirds (Aves: Apodiformes, Trochilidae) in functional and phylogenetic contexts. *Ornithol. Monogr.* **77**, 1–94.